Int J Earth Sci (Geol Rundsch) (2003) 92:228–254
DOI 10.1007/s00531-003-0311-5

ORIGINAL PAPER

Werner Schneider · Frank Mattern · PuJun Wang · Cai Li

Tectonic and sedimentary basin evolution of the eastern Bangong–Nujiang zone (Tibet): a Reading cycle

Received: 25 January 2002 / Accepted: 17 October 2002 / Published online: 28 March 2003

Abstract The ophiolite-bearing Bangong–Nujiang zone (BNZ) traversing central Tibet from east to west separates the Qiangtang block in the north from the Lhasa block in the south. Their stratigraphic development indicates that both blocks once formed a continuous continental platform until the Late Triassic. Following Late Paleozoic–Triassic rifting, ocean crust formed between both blocks during the Late Triassic creating the Dongqiao–Naqu basin (DNB) among other basins (Yu et al. 1991). The analysis of the rift flank sequences reveals that rifting was dominated by transtension. The basin was shortened by post-Mid-Cretaceous transpression. Thus, the overall basin evolution represents a Reading cycle despite some active margin processes which gave this cycle a special imprint. Major basin parts were preserved despite transpressional shortening suggesting that the eastern BNZ represents a remnant basin. Our understanding of the DNB solves the prior problem of viewing the BNZ as a Mid–Late Jurassic collisional suture although typical collision-related deformation, thickening, mountain building, as well as related molasse formation are lacking. Our model also explains the scattered linear ophiolite distribution by local transpression of remnant oceanic basin floor without having to consider problematic long range ophiolite thrusting.

Keywords Bangong–Nujiang zone · Basin analysis · Ophiolites · Reading cycle · Tibet

W. Schneider
Institut für Geowissenschaften,
Technische Universität Braunschweig,
Pockelsstraße 4, 38106 Braunschweig, Germany

F. Mattern (✉)
Institut für Geologische Wissenschaften,
Freie Universität Berlin,
Malteserstraße 74-100, 12249 Berlin, Germany
e-mail: fsap.mattern@t-online.de

P. Wang
Earth Sciences' College,
JiLin University,
JianSheJie Street 79, 130061 Changchun, P.R. China

C. Li
Department of Applied Remote Sensing,
JiLin University,
JianSheJie Street 79, 130061 Changchun, P.R. China

Introduction

The terranes of the Tibet plateau were accreted in a southward-younging fashion (Dewey et al. 1988; Mattern and Schneider 2000). In east Tibet, the Songpan–Ganzi terrane was accreted to the Kunlun during the Late Permian. The Qiangtang block was added onto the Songpan–Ganzi terrane at the Jinsha suture during the Late Triassic/Early Jurassic. In east Tibet, the Lhasa block was accreted to the Qiangtang block along the Bangong–Nujiang zone (BNZ) during the Mid–/Late Jurassic and in west Tibet during the Mid-Cretaceous (Yin and Harrison 2000). Finally, India was added onto the Lhasa block at the Zangbo suture during the Eocene.

The BNZ's tectonic interpretation is controversial. According to early interpretations by, for example, Pan and Zheng (1983), Zheng et al. (1984) and Coulon et al. (1986), the BNZ is a collisional suture. Girardeau et al. (1985) considered Late Jurassic to Early Cretaceous ophiolite obduction associated with long-range thrusting of >100 km. Xu et al. (1985) assumed a Mid-Jurassic collision. Pearce and Deng (1988) and Hsü et al. (1995) suggested that different ophiolite units of the BNZ may represent different types of lithosphere. However, their views of what may be forearc or backarc lithosphere are inconsistent.

It was also realized that the BNZ of the study area exhibits some features difficult to reconcile with a typical collision since pre- and postcollisional deformation are minor and evidence of mountain building and related molasse formation is lacking (Coward et al. 1988; Dewey et al. 1988). In western Tibet, it may have been a different situation (Murphy et al. 1997). Coward et al. (1988) also

discussed the problem of explaining the scattered ophiolite distribution via long-range thrusting.

Taner and Meyerhoff (1990) suggested that the BNZ resembles a rift, in part because both adjacent blocks display a similar geologic history. Subsequently, Yu et al. (1991) interpreted the BNZ as a pull-apart basin zone. Studying the stratigraphy of both the Qiangtang and Lhasa blocks that lack indication of rift-related thermal doming, as is typical for graben-type rifts, Mattern et al. (1998) concluded that the early Dongqiao-Naqu basin (DNB) was a strike-slip-dominated rift.

Based on our work on the DNB's sedimentary rocks and extensive compilation and synthesis of structural data, we outline the tectono-sedimentary basin evolution and put forward a new geodynamic model to overcome the above problems. The reader is encouraged to note similarities between the evolution of the DNB and a Reading cycle representing the strike-slip analogue to a Wilson cycle: transtensional rift–oceanized basin–transpressional belt (Reading 1980; Mitchell and Reading 1989). In equating radiometric ages with stratigraphic intervals and in quantifying time spans, we use the time table by Haq and van Eysinga (1998).

Geological background

The BNZ separates the northerly located Qiangtang block from the Lhasa block to the south (Fig. 1). Because the BNZ's terminations are ill-defined its length may exceed 1,700 km. The BNZ is generally 10 to 20 km wide. In the study area, however, its width measures 200 km. Yu et al. (1991) distinguished different ophiolite-bearing basins aligned along the BNZ, the DNB being one of them (Fig. 1). In the study area (Fig. 2), the BNZ is marked by Mesozoic ophiolites, including oceanic basement rocks that are scattered over a wide area. It is also characterized by Mesozoic shallow to deep marine sedimentary rocks as well as Meso-Cenozoic terrestrial strata representing the fill of the DNB. Mesozoic rocks may be intruded by granitoids and associated with volcanic rocks. The DNB also contains large blocks of continental basement, such as the 50-km-wide "Amdo massif" (Fig. 2), consisting of granite-intruded metasediments and granitic gneisses (Xu et al. 1985; Harris et al. 1988a). Ophiolites occur between these continental basement blocks. For a comprehensive regional bibliography see Yin and Harrison (2000).

In the following paragraphs some essential basic literature data concerning the Late Paleozoic to Tertiary lithofacies, paleontology, and paleogeography of the DNB and adjacent blocks are reviewed with the emphasis on the Jurassic to the Cretaceous/Tertiary.

Pre-Jurassic

The Lhasa block and the central and western Qiangtang block display a similar Carboniferous to Triassic shelf facies development (e.g., Bally et al. 1980; Leeder et al. 1988; Chang et al. 1989; Taner and Meyerhoff 1990). Whereas the Carboniferous is dominated by clastic deposits, carbonate accumulations became important during the Permian and Triassic. The faunal elements of both the Lhasa and Qiangtang blocks also reveal that a pre-Jurassic shallow marine platform existed (Smith and Xu 1988). Minor terrestrial intervals occur in the predominantly marine Late Permian and Triassic successions (Fig. 3).

The platform was affected by Permian to Early Mesozoic rifting. Late Triassic to Early Jurassic normal faults of the Qiangtang block were active during southward subduction along the Jinsha suture (Kapp et al. 2000). Permian volcanism within the Qiangtang and Lhasa blocks was attributed to extensional tectonism of

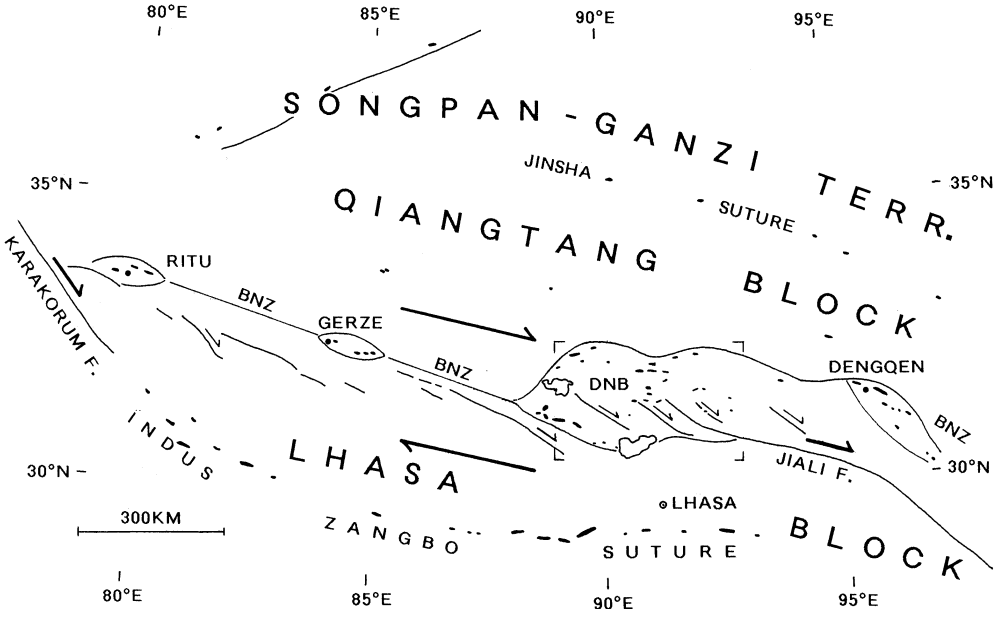

Fig. 1 Tibetan ophiolites (*black*; after Kidd et al. 1988) and basins (after Yu et al. 1991) along the BNZ as well as the Miocene to present dextral simple shear zone with left-stepping, en échelon, and WNW-trending lateral escape faults (after Armijo et al. 1983; Pêcher 1991) that do not enter the adjacent blocks. The western BNZ is much narrower. *Box* represents study area

Fig. 2 Simplified geological map of the study area (modified after Kidd et al. 1988). Parts of the Lower Cretaceous outcrop zone SE of Lunpola, as shown on the map by Kidd et al. (1988), actually represent conglomeratic mass flow deposits belonging to the upper segment of the Jurassic sequence

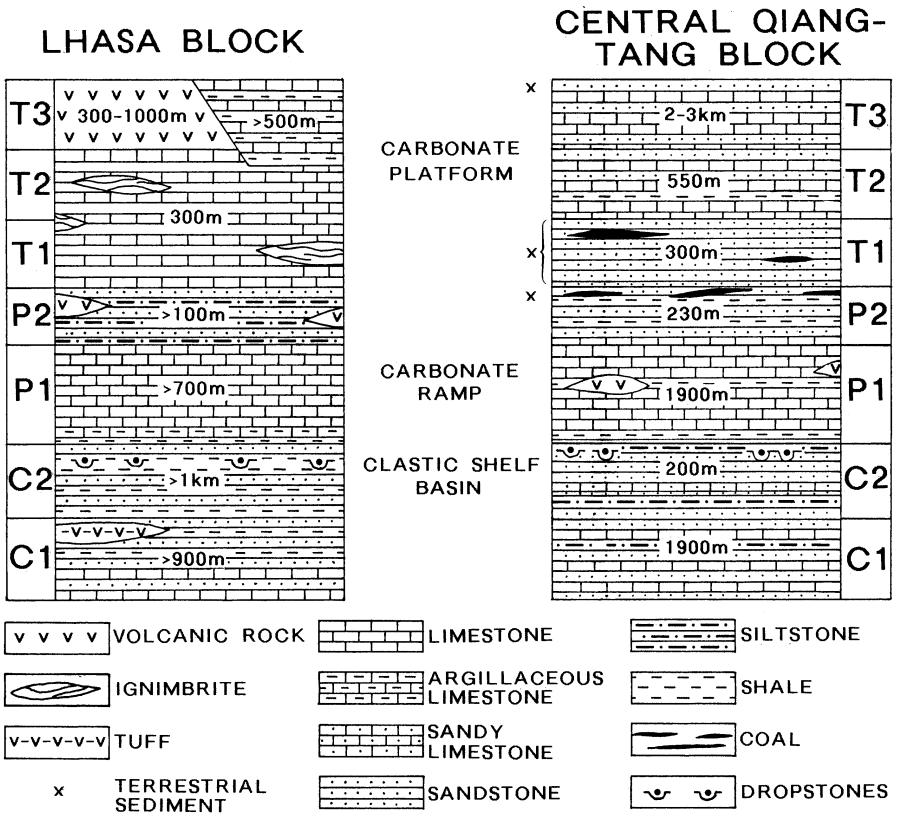

Fig. 3 Pre- and synrift rift flank successions of the Lhasa block and central Qiangtang block with similar shallow marine facies and sparse terrestrial deposits (sources: Leeder et al. 1988; Yin et al. 1988; Taner and Meyerhoff 1990)

backarc or rift affinities. Rifting led to fragmentation of the Triassic Lhasa carbonate platform and accounts for observed bathymetric differences (Leeder et al. 1988). Permian volcanic rocks of the northern Qiangtang block display a transitional composition between tholeiitic and alkaline, and were interpreted as having formed within attenuated continental lithosphere during rifting by Pearce and Mei (1988). According to Chang et al. (1989), Late Triassic volcanic and pyroclastic rocks of the north-central Lhasa block reflect initial basin opening.

The stratigraphic analysis of the Lhasa and Qiangtang blocks reveals that their overall character remained that of a marine platform during rifting (Fig. 3). There is no evidence for a major rift-related thermal Cloosian dome (Mattern et al. 1998). The Scythian is the main terrestrial interval. Because Scythian terrestrial deposits are restricted to only the Qiangtang block and the Scythian is of only short duration (Harland et al. 1990: 4 million years; Haq and Van Eysinga 1998: 5 million years), we don't attribute the Scythian emergence to a major, rift-related regional uplift. Minor Late Triassic terrestrial intervals of the Qiangtang block probably resulted from uplift related to the Songpan–Ganzi belt/Qiangtang block accretion. As of the Late Triassic, major facies differences were recognized on both sides of the BNZ by Chang et al. (1989), who concluded that the Lhasa and Qiangtang blocks formed one continuous platform until the Late Triassic when the DNB opened between them. As a result, oceanic crust formed before the Jurassic (Sengör 1981a; Wang et al. 1987; Taner and Meyerhoff 1990). Because rifting evidently occurred, but was not accompanied by major pre- and/or synrift doming, as is typical for graben-type rifts, we concluded that Triassic continental separation was due to transtension (Mattern et al. 1998).

Jurassic

The Qiangtang block's Jurassic carbonates are helpful in defining the block's southern margin because they contrast sharply with the DNB's predominantly fine-grained clastic Jurassic rocks. Thus, the delineation between the Qiangtang block and the DNB is straight forward. Deposition on the DNB's northern slope is characterized by olistostromes and large olistoliths of Qiangtang provenance. The southern slope lacks such deposits and appears more stable. We interpret the northern slope, therefore, as relatively steep and the southern slope as comparatively gentle.

The Qiangtang block lacks Early Jurassic deposits except for the block's easternmost part (Smith and Xu 1988; Yin et al. 1988). Between Yanshiping and Amdo, the Mid- and Late Jurassic is represented by the more than 5-km-thick Yanshiping Group (Yin et al. 1988), consisting of siliciclastic and carbonate rocks displaying the transition from fluvial sediments in the north to marine carbonates in the south. According to Leeder et al. (1988), coastal plain/sabkha deposits mark the transition from the

northern to the southern facies realm of the Qiangtang block. The Jurassic of the Qiangtang block may include mafic and silicic volcanic rocks (e.g., Kidd et al. 1988).

Yin et al. (1988) listed a variety of fossils (dinoflagellates, bivalves, gastropods, brachiopods, and ammonoids) representing the Bajocian and Upper Jurassic of the Qiangtang block.

A significant portion of the DNB's basin fill is represented by fine-grained, marine, siliciclastic deposits called "Lake Area Flysch". The Lake Area Flysch is very thick (Yin et al. 1988: >4 km; Yu et al. 1991: >9 km). In the south (e.g., Baingoin area), which seems to lack Early to Mid-Jurassic strata, the thickness of the Jurassic is much smaller (Yin et al. 1988: 700 m). Common and characteristic is hemipelagic, black shale alternating with clay, silt and sandstone. There are subordinate intercalations of allochthonous and autochthonous limestone whose faunal spectra indicate a shallow shoreface as well as deep offshore environments (Leeder et al. 1988; Yin et al. 1988).

Among the DNB's carbonates there are autochthonous shallow water carbonates (e.g., SW Lunpola, Leeder et al. 1988) and biocalcarenites containing siliciclastic debris. According to Yin et al. (1988), neritic Early Jurassic deposits occur along the southern and northern margins of the Lunpola basin. A marine reefal limestone facies was described NW of Dongqiao by Girardeau et al. (1984), Chang et al. (1986), and Leeder et al. (1988). Near Dongqiao, olistoliths display a shallow marine fauna of corals, stromatoporoids, and echinoderms, which matches that found in Kimmeridgian to Valangian? reef limestones south of Lunpola (Smith and Xu 1988).

The Jurassic of the DNB/Lhasa block commonly displays local unconformities, lateral facies changes within short distance, and great thickness variations. Yin et al. (1988) summarized the vertical facies change of the Lake Area Flysch that reflects environmental transitions from pelagic to continental slope. In addition, they reported a facies change from the flysch of the lake area eastward to the Naqu area, south of the Amdo massif, where the Mid-Jurassic is represented by red conglomerate and the upper Mid-Jurassic comprises oolitic limestone, mudstone, and bioclastic limestone interlayered with andesite and volcanic breccia. The basal Upper Jurassic consists of red and gray conglomerates, granitoid conglomerates, and pebbly flysch sandstone.

Biostratigraphic data on the DNB are incomplete. Lower Jurassic ammonoids and plants have been reported by Wang (1983), Wen (1984), and Wang and Sun (1985). Wang (1984) and Li (1986) dated Radiolaria from cherts associated with flyschoid deposits and ophiolites as Upper Jurassic. From the Lake Area Flysch occurring in the Naqu–Dongqiao–Gyanco–Lunpola region (Yin et al. 1988), Girardeau et al. (1984) listed an Aalenian fauna from the Gyanco area represented by *Gutnicella* (*Lucasella*) *cayeuxi, Haurania* sp. and *Nauticulina* sp. and a Malm fauna with gastropods and *Sequania* sp. from the Dongqiao area. Smith and Xu (1988) listed *Cladocoropsis* sp., nerineid gastropods, and other shallow marine faunas confirming Upper Jurassic for the Dongqiao area. For further paleontologic age data see Smith and Xu (1988), Yin et al. (1988), Chang et al. (1989), and Taner and Meyerhoff (1990).

Cretaceous

Cretaceous strata only occur on the DNB/Lhasa block (Kidd et al. 1988). There is no uniform lithostratigraphic development due to facies changes occurring at short lateral and vertical distances and due to hiatuses within terrestrial/volcanic successions. Fossils are sparse.

Lower Cretaceous

The more than 1.3-km-thick Duba Formation mainly comprises terrestrial siliciclastics intercalated with some calcareous sandstone beds bearing *Orbitolina* sp., indicating a marine influence (Yin et al. 1988). The fine-grained terrestrial clastics are of flood plain aspects, the coarser ones are of sheet flood and channel origins (Leeder et al. 1988).

The Duba Formation is overlain by the 700–900-m-thick marine Langshan Formation in the Baingoin-Nam Co Lake area (Kidd et al. 1988; Leeder et al. 1988; Yin et al. 1988). Between the Langshan Mts. in the south and the Lunpola area, beds of the Duba Formation interfinger with their lateral equivalents of the northern Xiaqiong Formation (Yin et al. 1988).

At the type locality in the Langshan Mts. (Duba region), the >200-m-thick Langshan Formation exhibits massive rudist limestone (patch reefs) alternating with orbitolinid-bearing mudrocks, which are overlain by fine-grained clastics passing into a limestone/mudrock sequence (Leeder et al. 1988).

The formation's rich fauna of corals, foraminifers, brachiopods, gastropods, and bivalves provide a reliable biostratigraphy within the Aptian–Albian, possibly also Cenomanian (Smith and Xu 1988; Yin et al. 1988). The formation was deposited in very shallow marine environments with rudist patch reefs and back reef lagoons (Leeder et al. 1988).

South of Lunpola, >300-m-thick Xiaqiong Formation overlies Kimmeridgian strata of bioherms followed by dolomitic siltstones, which may extend to the Jurassic/Cretaceous boundary (Leeder et al. 1988). According to Leeder et al. (1988), the lower part of the formation consists of thickening-up cross-bedded sandstones with common erosional surfaces alternating with mudstone representing fluvio-distributary channel sediments. The following strata are characterized by siltstone and fine-grained sandstone with periodic cross-bedded sandstone beds of possible floodplain origin (Leeder et al. 1988). Yin et al. (1988) also mentioned intercalated amygdaloidal basalt. Towards the top, marine limestones bearing oysters and Aptian/Albian orbitolinids, follow an exposure gap (Leeder et al. 1988). These beds have

formally been included in the Xiaqiong Formation, which passes upward into the Langshan Formation (Yin et al. 1988). Because an Aptian/Albian age is also known for the marine, orbitolinid limestones of the Langshan Formation (Jaeger et al. 1982; Yin et al. 1988), it is practical to assign them to the Langshan Formation as we did in our figures. Foraminifers and gastropods definitely indicate Aptian and Albian age (Smith and Xu 1988). It is unclear whether the Langshan Formation includes Maastrichtian deposits; the latest marine fauna appear to be Albian (Cenomanian?) orbitoline foraminifers (Smith and Xu 1988).

Upper Cretaceous and Tertiary

Stratigraphic charts show a lack of post-Cenomanian or post-Turonian Upper Cretaceous rocks (Smith and Xu 1988; Yin et al. 1988) although Campanian volcanic rocks (Coulon et al. 1986) occur in the region and are associated with red beds (Pearce and Mei 1988). The knowledge of the Upper Cretaceous deposits is poor. They are mapped by Kidd et al. (1988) as "Kt" along with the Duba Formation and Paleogene. Thus, it is uncertain to what extent field observations pertaining to "Kt rocks" actually concern the Upper Cretaceous. In the north, "Kt beds" display an abrupt distributional boundary because they are absent on the Qiangtang block, but cover the northern DNB.

The combined thickness of Paleogene and Neogene deposits (all terrestrial clastic sediments) may reach 3.8 km as in the case of the Lunpola basin (Yin et al. 1988).

Sedimentology of the Jurassic, Cretaceous, and Tertiary (field data)

A synopsis of our observations and interpretations is summarized in Fig. 4.

Qiangtang block, Jurassic

Along the road from Golmud to Amdo, a 3,700-m-thick Mid- to Upper Jurassic section was studied near Amdo at location #11 (Fig. 2), displaying the following lithofacies units. At the base, fluvio-deltaic yellowish and reddish sandstones, as well as conglomerates of some tens of meters in thickness, occur. Among the conglomerates, sparse clast imbrication indicates S-directed transport. The conglomerates are overlain by yellowish and gray, thin- to medium-bedded, fine-grained, well-sorted and horizontally laminated sandstones, which are a few meters thick (facies type Sh of Miall 1985). The next unit consists of medium- to thick-bedded, fossiliferous, bituminous, micritic, shallow marine limestone of several hundreds of meters thickness. The limestone is overlain by several tens of meters of thick, red and green, fine-grained, plant debris-bearing sandstone with partly conglomeratic fining-up channel fill sequences ("Sm" to St to Sp to Sr of Miall 1985). The following several hundred-meter-thick unit is composed of black shale and bituminous micritic limestone. The top of the section is represented by a thick-bedded, more than 2 km thick, bituminous marl and limestone unit containing a marine fauna of ammonoids and bivalves as well as plant debris. No volcanic rocks were observed.

Along the same road, NE of Amdo, an approximately 100-m-thick section of sheared and brecciated bituminous limestone and marlstone is exposed (location #10). The position of this section is close to the tectonic boundary between the Qiangtang block and the DNB.

The Jurassic represents a near-coastal environment where fluvio-deltaic sediments interfinger with the foreshore and, towards the top and south, increasingly with shoreface conditions of an open sea (compare Leeder et al. 1988; Yin et al. 1988). Thus, this Mid–Late Jurassic environment can be considered a paralic molasse that accumulated as a result of the Qiangtang block's accretion to the Songpan–Ganzi terrane. In agreement with this is the lack of Early Jurassic deposits over much of the Qiangtang block, reflecting accretion-related compression, uplift, and erosion. A relatively high northern elevation is still indicated for the Mid- to Late Jurassic by the above mentioned facies transition from terrestrial in the north to marine in the south and the S-directed transport.

DNB/Lhasa block, Jurassic

The central part of the study area, the so-called "Lake District Area", shows a significant N–S facies change of Jurassic strata (Figs. 5, 6, and 7). Immediately south of the Qiangtang block, the sediments are partly olistostromatic (location nos. 4 and 17) followed southward by deep marine pelite/chert-dominated facies (location nos. 1, 2, and 5). Farther south, shallow marine pelecypod-bearing deposits to intertidal sediments are characteristic (location #13).

In the eastern part of the study area, the large crystalline block of the Amdo massif occurs within the DNB, separating ophiolite occurrences to the north and south. This points to the massif's role as a source area throughout the Jurassic and Cretaceous (Fig. 7) and a facies-controlling factor (e.g., location nos. 7 and 8). The Amdo massif and its surroundings serves to illustrate that the DNB was not a simple basin, but rather a mosaic of sub-basins separated by continental structural highs.

In the following paragraphs, characteristic type sections across the DNB will be described and interpreted regarding their sedimentary environments (land, land/basin slope transition, basin slope, basin, shallow marine; compare Figs. 5, 6, and 7).

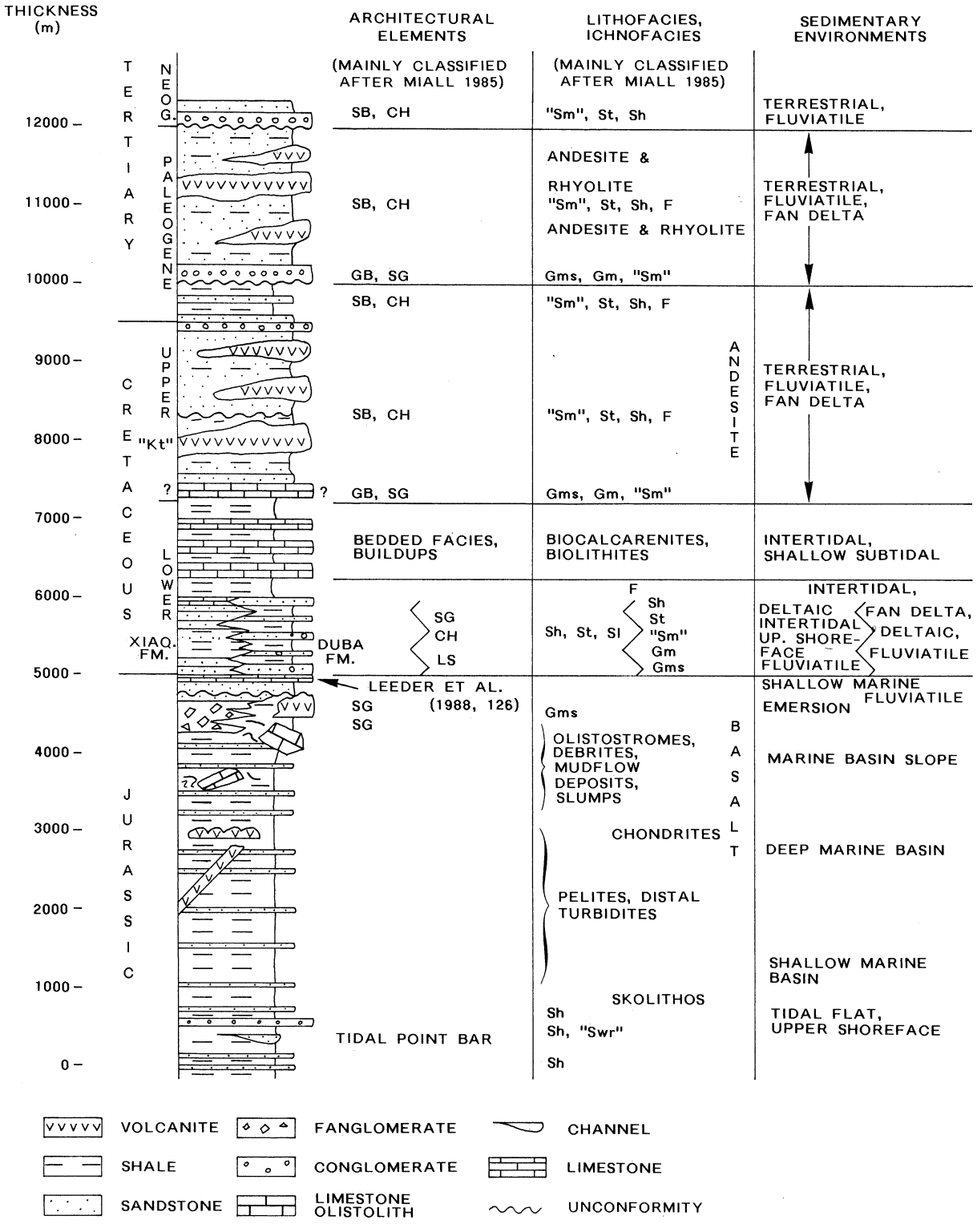

Fig. 4 Synopsis of the lithostratigraphy and facies of the DNB's Jurassic, Cretaceous, and Tertiary deposits from our own observations. Positions of Cenozoic unconformities possibly vary

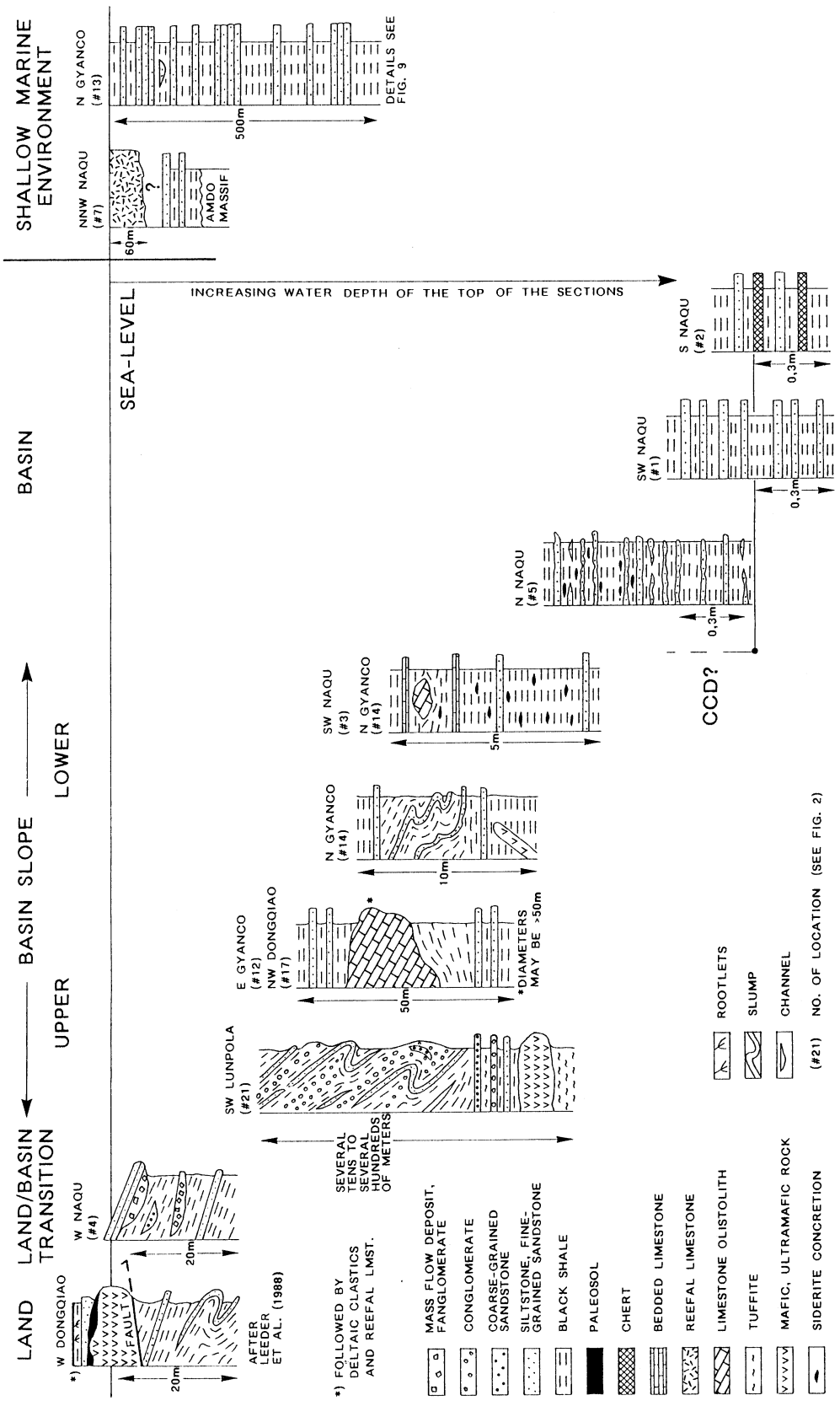

Fig. 5 Schematic type sections of representative Jurassic lithofacies assemblages in different sedimentary environments of the DNB. Note the interpreted relative paleobathymetry

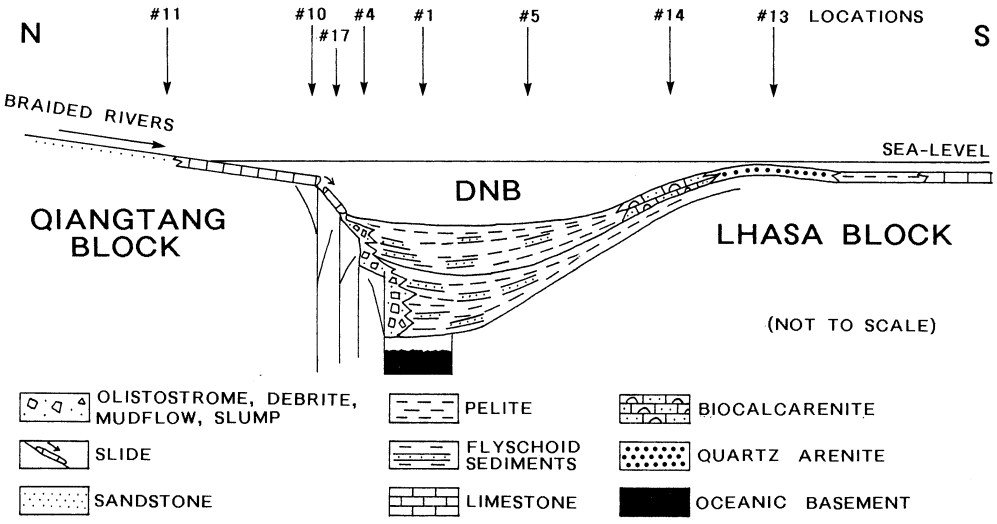

Fig. 6 Schematic cross section of the asymmetric DNB showing Mid–Upper Jurassic facies distribution and approximate relative paleobathymetric positions of some investigated sites

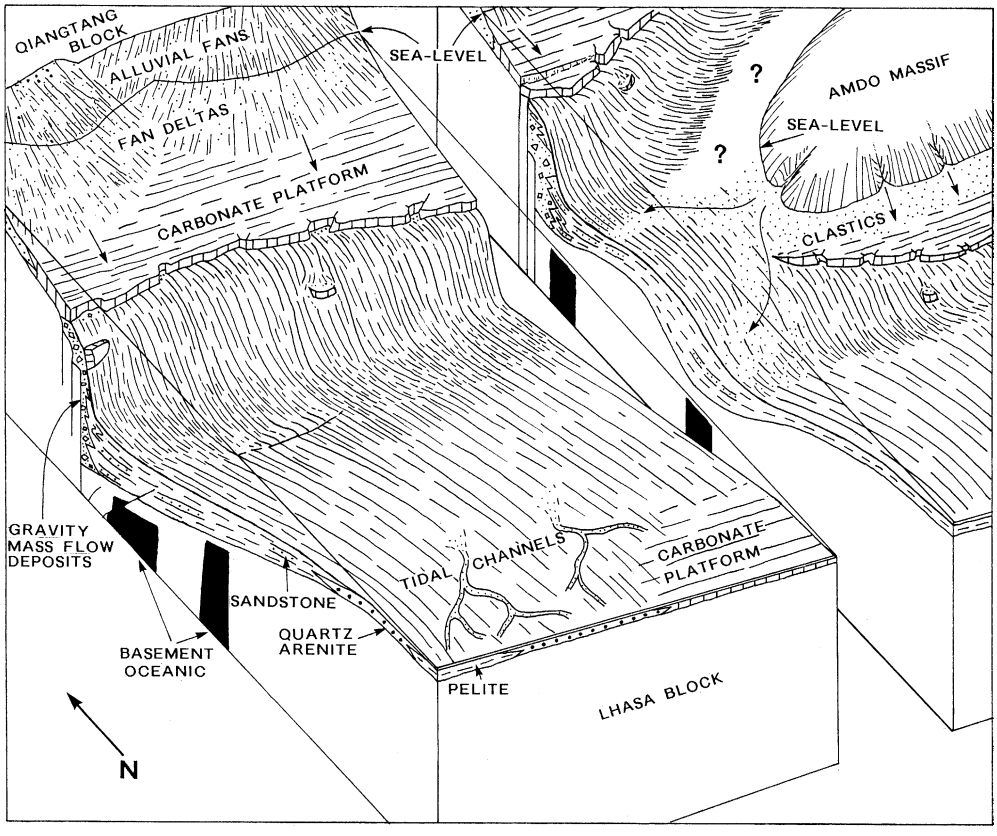

Fig. 7 Generalized paleogeographic sketch of the DNB for the Middle to Upper Jurassic showing the tectofacies pattern of the DNB. Note the basin asymmetry in N–S direction and related facies distribution. Olistostromes, debrites, mudflow deposits, and slumps occur at the steep northern basin slope, deep-water sediments (partly turbiditic), and zones of autochthonous oceanic crust in the center of the basin and shallow-water environments at the gentle southern basin slope

Land

The type section for the terrestrial sedimentary environment is located west of Dongqiao (Fig. 5; Girardeau et al. 1984; Chang et al. 1986; Leeder et al. 1988; Smith and Xu 1988), where slumped pelitic rocks are overthrust by serpentinized ophiolites. Local emergence of the basin floor is indicated by paleosol horizons above a thrust, which are overlain by fluvial sandstone, rootlet-bearing pelite, and transgressive shallow marine carbonates containing the Tithonian alga *Cladocoropsis* (Smith and Xu 1988). This type of section is of tectonic significance and is discussed later.

Land/basin slope transition

A quarry west of Naqu displays the type section for the land/basin slope transition (location #4; Figs. 5 and 8E), with dark pelites in which highly disorganized, lenticular mass flow deposits are interbedded. The thickness of the latter ranges from several meters to decameters. These beds represent polymictic breccias with mainly intraformational clasts of black shale, chert, siltstone, and sandstone, whose long axes may exceed 1 m. In the upper section is a transition to fluvial fanglomerates and horizontally-bedded, well-sorted plant-bearing sandstones displaying copper mineralization. The lenticular beds either represent channel fills in a fluvial/subaquatic environment and/or scours generated by strong current action, or slump scars within fine-grained marine sediments at the uppermost part of a mobile basin slope.

In another quarry, 400 m north of location #4, close to a local nunnery, an isolated yellow, fluvial allochthonous massive sandstone body containing granitoid debris appears embedded in pelites. This 10-m-thick deposit very likely represents a channel fill.

These observations correspond to those of Yin et al. (1988), who noticed the influence of the Amdo massif on the sedimentary development of this region. They observed a Mid-Jurassic red conglomerate directly overlying the metamorphic rocks of the Amdo massif and that the base of the Upper Jurassic consists of red and gray conglomerates as well as granitoid debris-bearing conglomerates (compare Fig. 7).

All these occurrences are located in the same region, and represent a transitional or shallow marine water facies. The clastic rocks, as well as Mid-Jurassic oolitic and bioclastic limestones, andesites, and volcanic breccia, reflect a facies change from the Lake Area Flysch in the west towards the east. This change was partly controlled by the proximity of the Amdo massif, representing a shallow marine or even supratidal environment.

Basin slope

Type sections of the DNB's northern basin slope were studied between Amdo and Qiling Co (location nos. 3, 12, 14, 17, and 21). The sections display trains of shallow marine carbonate olistoliths with long axes, up to 100 m, embedded in Jurassic shale (Figs. 5 and 8C). The olistoliths, composed of bituminous, micritic limestones, and bearing a Jurassic shallow marine fauna, match the limestone types of the Qiangtang block near Amdo (compare location #11). They are absent in the southern parts of the DNB.

In the sections of at location nos. 12, 14, and 17 the dark shale alternates with coquina beds and thin-bedded allodapic limestones (Fig. 5). The olistoliths occur in olistostrome or debris flow deposits. They are especially noticeable between Amdo and Naqu, as well as around Dongqiao. Mudflow deposits and slumps may also be present. This facies indicates that the transport path to the depositional site was a relatively steep slope. The instability of slope sediments and the detachment of large limestone blocks from the northern basin margin may point to seismic activity (Fig. 7).

At the southern margin of the Lunpola basin (location #21), at the top of the Jurassic deposits, olistostromes with large-scale soft sediment deformation are exposed (Fig. 5). The olistostromes include black shales, fine-grained siliciclastic rocks, chert, and conglomerates.

The pebbles of the conglomerate represent a polymictic lithic association of slate, siltstone, sandstone, chert, quartzite, marl to limestone, and bituminous limestone displaying varying roundness (Fig. 8D). The components are supported by a bituminous, pelitic matrix. Among centimeter-sized quartzite and chert pebbles the roundness value is rather high, indicating significant reworking in fluvial and/or coastal environments. Because the bituminous limestone components compare closely to the above described olistoliths, extraformational constituents (limestone) and intraformational components (e.g., siltstone, sandstone) were intensely mixed. Towards the base of the section we found an association of pillow lavas, tuffites, intraformational breccias, and mass flow deposits. However, because of the reworked conglomerate components, there is indirect evidence for the terrestrial influence on the depositional development within the basin.

At locations #3 and #14, the black shales are intercalated with centimeter- to decimeter-scale siltstone/fine-grained sandstone beds (D2.3 of Pickering et al. 1989), as well as centimeter-thick bituminous coquina beds that appear to be turbiditic. The latter are made up of crinoid and brachiopod debris. Together with small limestone olistoliths, these allochthonous carbonate rocks indicate a rather distal position at a relatively deep segment of the paleoslope.

Basin

The studied basinal type sections are located around Naqu (locations nos. 1, 2, and 5). North of Naqu, at location #5, road outcrops exhibit a rhythmic alternation of black shale and siltstone. The warve-like sediments show regular to irregular bedding. The facies compares with type D2.2 of Pickering et al. (1989). The bed thickness of sandstones is at the millimeter to centimeter scale. Such sequences are several decameters thick and frequently bear marly siderite nodules up to 30 cm in length, suggesting some oxygen deficiency in the depositional environment (see Füchtbauer and Richter 1988). This, the lack of high-energy depositional events and the continuous deposition of fine-grained materials, make a quiet and rather deep basin environment likely.

As shown in road outcrops SW of Naqu (e.g., location #1, Fig. 8B), the Jurassic is generally dominated by cyclic alternation of black shale, thin-bedded siltstone, and fine-grained sandstone (mainly facies type D2.3 of Pickering et al. 1989). The sandstone beds' thickness is at the

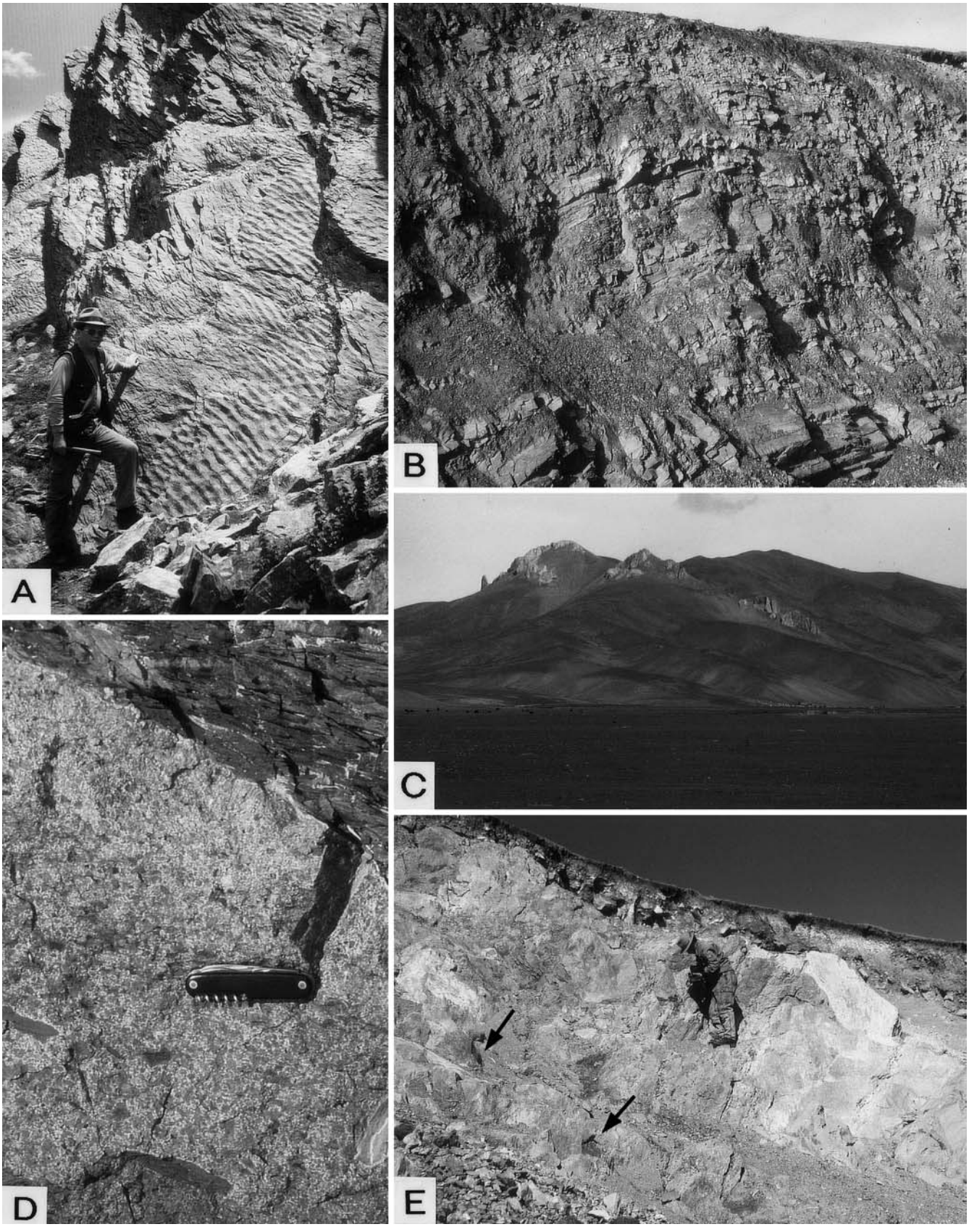

Fig. 8 A–E Jurassic sedimentary rocks of the DNB. **A** Cross and oscillation ripple marks of intertidal deposits at the base of the quartzites at Jang Co Lake (location #13). **B** Typical sequence of dark mudstone, siltstone, and sandstone of the Lake Area Flysch. Roadside outcrop south of Naqu (location #1). **C** Large limestone olistoliths in a pelitic matrix between Naqu and Gyanco (location #12). **D** Chert-rich breccia intercalated in alternating bituminous siliciclastic deposits and pillow lavas from the southern margin of the Lunpola Basin (location #21). **E** Debrite with intraformational dark shales (*arrows*) in the top of the Jurassic sequences west of Naqu (location #4)

centimeter to decimeter scale. Horizontal bedding is typical. These sandstones are Bouma base-missing turbidites, generally lacking $T_{a–c}$. A few flute casts indicate transport towards the west and south. Sections of this type measure up to several hundred meters and may be associated with synsedimentary basalt lavas and/or dikes. This facies type lacks carbonate contents and, thus, leads us to assume a deep, quiet, mostly anoxic environment. The more frequent occurrence of sandstone beds, in comparison to location #5, may indicate a closer source area for the siliciclastic debris.

At location #2, south of Naqu, several decameter-thick sequences of alternating black shales, thin beds of siltstone, fine-grained sandstone (D2.3 of Pickering et al. 1989), chert, and chert breccias are exposed. Allochthonous coquina beds are absent in this calcite-free facies type, which formed in a low-energy, anoxic and deep marine environment. Whether the radiolarian-bearing cherts were deposited below the CCD is uncertain.

Shallow marine environment

The type section (Fig. 5) at the northern shore of Jang Co Lake, north of Gyanco, displays a 500-m-thick sequence of well-exposed weakly metamorphosed dark shales, siltstones, fine- to medium-grained sandstones, and quartzites (location #13; Figs. 8A and 9). The sandstones exhibit mainly horizontal bedding, partly wave and cross ripples of low wavelength (Fig. 8A), *Skolithos*, and undeterminable grazing and resting traces. Sandstones with conglomeratic lag deposits, consisting mostly of reworked black shales, represent channel fills within the black shales. White quartzites occur close to the top of the section. The lithofacies, sedimentary fabrics, and trace fossils indicate an intertidal to shallow subtidal environment with tidal channels. The quartzites represent a mature coastal depositional environment. Coquina beds with bivalve and brachiopod shells overlie this sequence and mediate to the overlying Lake Area Flysch. The whole sequence reflects retrogradation of sandy foreshore and shoreface sediments, perhaps related to the earliest stage of basin subsidence in its southern realm during the Jurassic.

The type section between Naqu and the Amdo massif displays massive, poorly-bedded reefal limestones at a 60-m-high cliff (location #7). The bituminous biolithites and biopelmicrites contain a shallow marine fauna of stromatoporoids (Fig. 10A), crinoids, brachiopods, gastropods, corals, and benthic foraminifers whose exact age is unknown. The biostromal facies at this location demonstrates that the southern foreland of the Amdo massif was located in a shoreface environment. Whether the Amdo massif had emerged at that time is uncertain. A similar facies was described for the Dongqiao area by Girardeau et al. (1984), Chang et al. (1986), and Leeder et al. (1988).

The DNB/Lhasa block's flyschoid Jurassic is not a classic turbidite sequence because hemipelagites predominate. Turbidites are usually of the Bouma base-missing type. Coarse, high-concentration turbidity current deposits are absent. Hemipelagic sedimentation and alternating hemipelagites and "distal" turbidites (E and D facies classes sensu Pickering et al. 1989) are reminiscent of deep lake sedimentation. Among other types of gravity mass-flow deposits, olistostromes have a special impact on the lithofacies and lithostratigraphy. There is also evidence for shallow marine, fauna-bearing carbonates, *Skolithos* ichnofacies of foreshore environments, and even local paleosols.

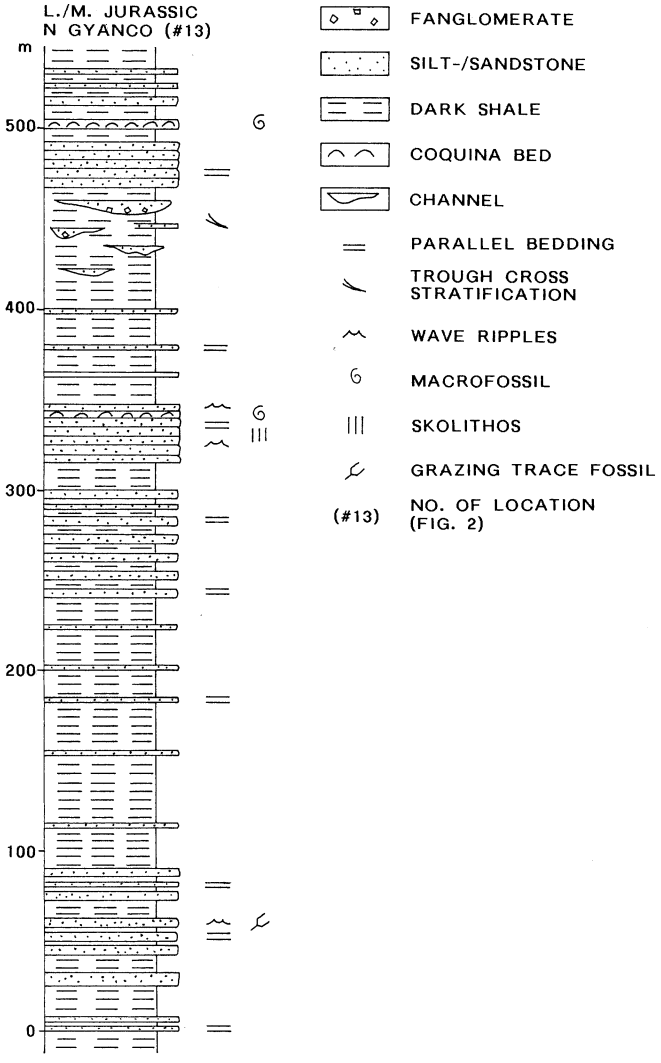

Fig. 9 Neritic Jurassic clastic sediments of the DNB: lithostratigraphy of foreshore/shoreface deposits at the northern shore of Jang Co Lake (location #13)

Figure 6 shows a model of the DNB for the Mid- to Upper Jurassic, emphasizing its asymmetry and related facies distribution. Olistostromes, debrites, mudflow deposits, and slumps occur at the steep northern basin slope, deep-water sediments and zones of autochthonous oceanic crust occur in the center of the basin, and shallow water deposits are found at the gentle southern basin slope.

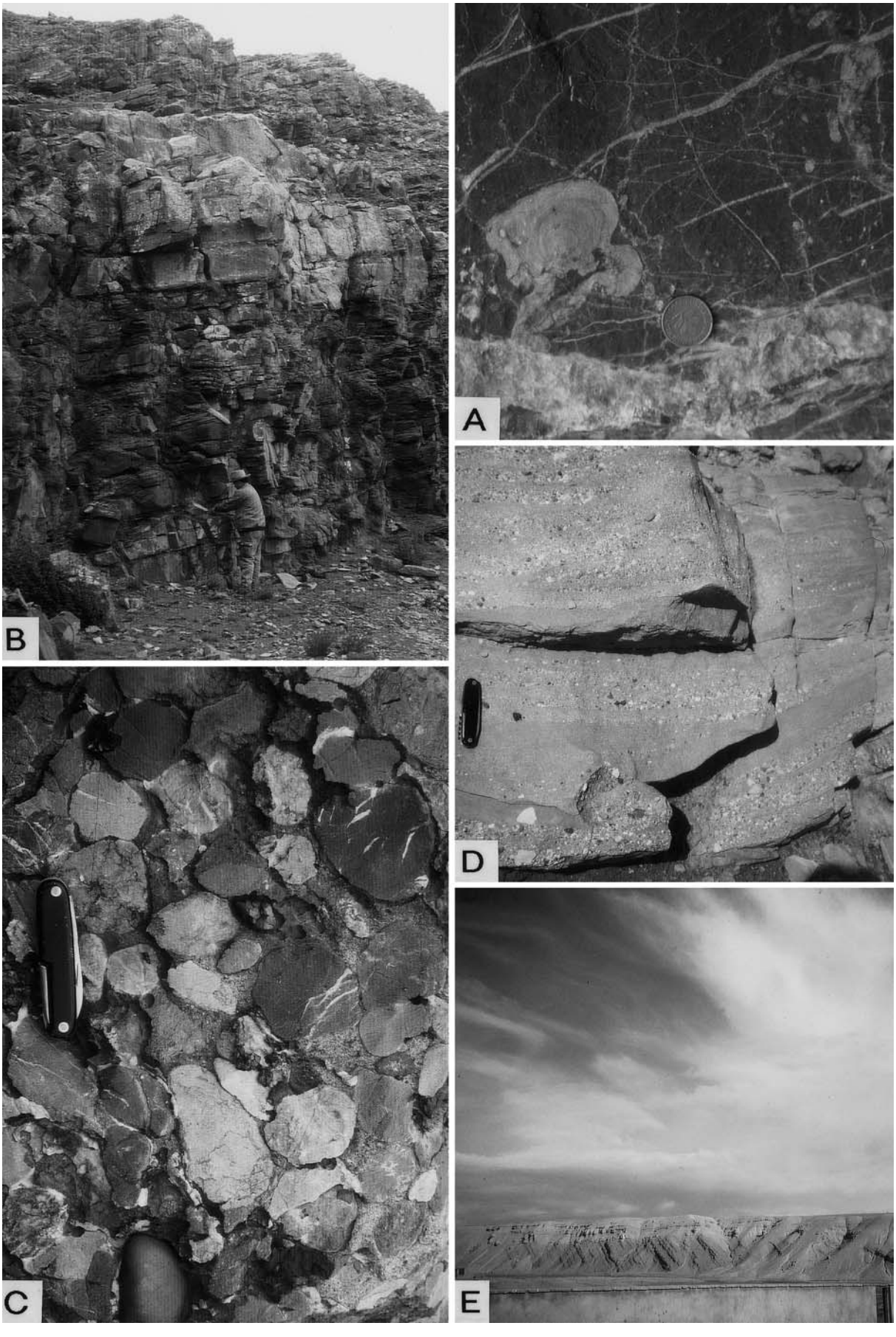
A
B
C
D
E

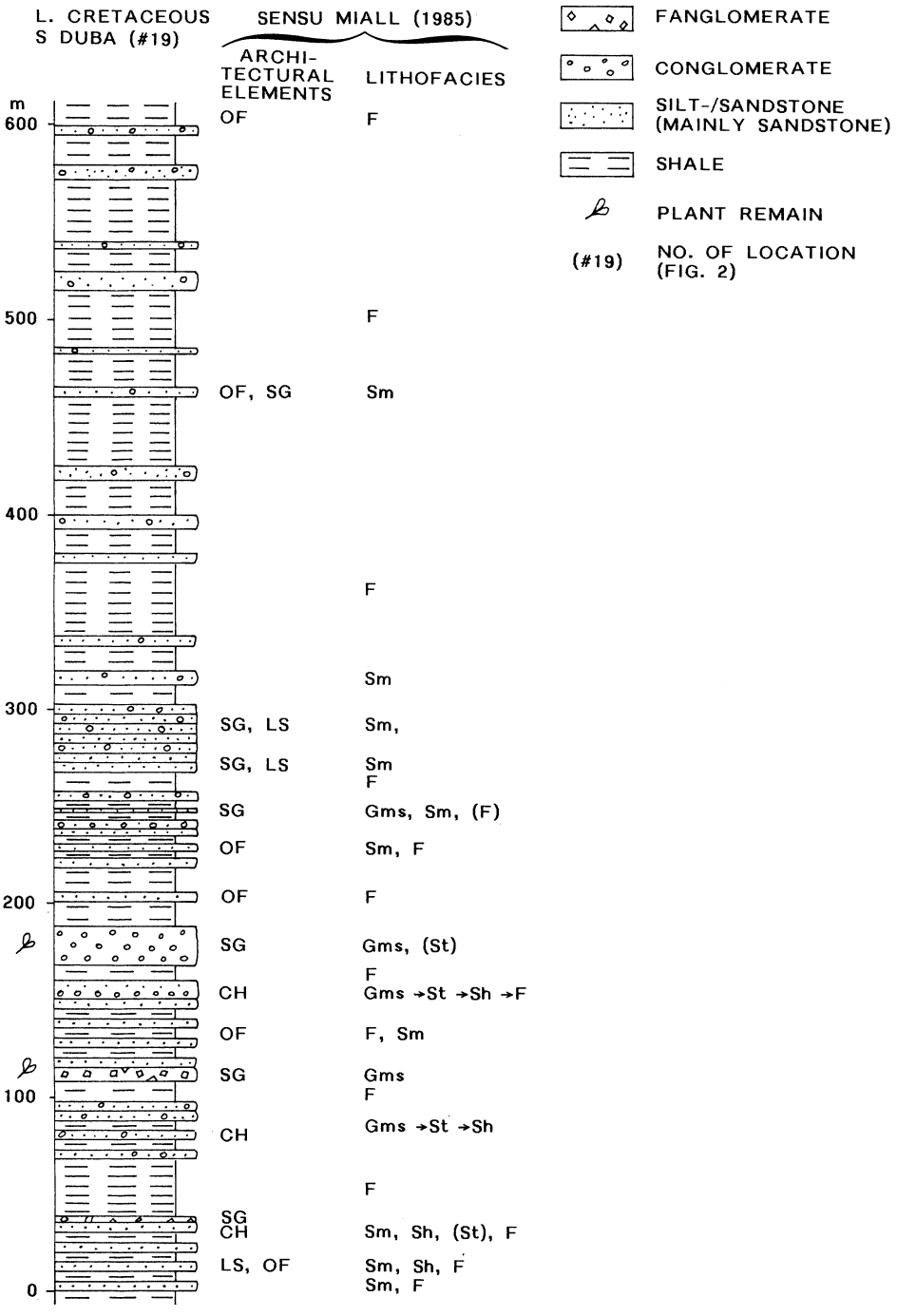

Fig. 11 Lithostratigraphy and facies of the Lower Cretaceous Duba Formation at location #19

Fig. 10A–E Sedimentary rocks of the DNB. **A** Bituminous, stromatoporoid-bearing biomicrite south of the Amdo massif (location #7). Diameter of *coin*: 2.1 cm. **B** Horizontally bedded "Kt sandstone" (Sh, Miall 1985) and conglomerate at Duba (location #20). **C** "Kt conglomerate" mainly composed of limestone clasts derived from the Langshan Formation and the Qiangtang block's Jurassic, and less frequently of chert, quartzite, and dark Jurassic sandstone from the BNZ (location #20). **D** Channel fill with trough cross-bedding (CH, St, Miall 1985) intercalated with distal fan delta and muddy playa deposits of presumably Upper Cretaceous/Tertiary age 8 km north of Nima County Town. **E** Tilted Paleogene red beds unconformably overlain by clastic Neogene at Nima County Town

Lower Cretaceous

The mountains of the Duba region expose more than 800 m of the Duba formation (location #19; Fig. 11). The formation's overall reddish lower part (ca. 150 m) mainly consists of reddish, yellowish, and greenish sandstone and a few conglomerate/fanglomerate beds all intercalated with red, violet, and green pelites. The sandstone/pelite ratio is 4:1. The thickness of the medium- to thick-bedded, plant-bearing sandstone units can reach 25 m. Despite their textural and compositional immaturity,

some pebbles are well rounded. While the coarse clastics represent the fluvial part of a terrestrial fan delta, the pelites represent adjacent back-swamps and/or coves.

In the middle part of the formation (ca. 450 m thick) violet, green, and gray colored rocks are more common. The number and thickness of the medium- to thick-bedded, coarse-grained clastics decreases towards the top of the section, showing an increasing predominance of green pelites. Up to 1-m-thick conglomerate and fanglomerate beds are volumetrically of minor importance.

According to Miall's (1985) nomenclature, laminated sand sheets (LS), as well as disorganized conglomerates, fanglomerates, and sandstone (SG), predominate as architectural elements in the lower and middle part of the formation in comparison to channels (CH)

The polymictic conglomerates contain components of shale, limestone, quartzite, and granite, as well as mafic and acidic to intermediate volcanic rocks of different degrees of roundness. Occasionally, there are fining-up sequences (Gms to "Sm" to St to Sh to F) within shallow (1–2 m) channels, which occur in relatively thick (up to 35 m) shale intervals. There are also 25-m-thick terrestrial sandflat deposits.

The overall nature of this fining-up succession is that of a fan delta exhibiting a retrogradational trend. A few paleocurrent measurements on St units provide evidence for a SW-directed transport, similar to that detected by Leeder et al. (1988).

The upper Duba Formation (ca. 250 m thick) consists of dark pelites and black shales intercalated with a few thin sandstone beds. This facies marks the beginning transgression of the Aptian Sea.

Upper Cretaceous

Numerous outcrops show that the thick (>3 km) "Kt rocks" accumulated as alluvial fans and terrestrial fan deltas. The red beds, south of Dongqiao at location #16, are characterized by the lithofacies types Gms, "Sm", Sh, and F sensu Miall (1985). They contain mainly andesite and some reworked Jurassic sedimentary material. West of Duba, at location #20, poorly organized sediments predominate, although 15 conglomerate/sandstone cycles with fining-upward trends are present (Fig. 10B; Gms, "Sm", St, Sh, F of Miall 1985). Six paleocurrent measurements from St units (trough cross stratification) indicate westward transport. In the upper part of the 1-km-thick section, up to 20-m-thick conglomerates occur (Fig. 10C). At location #20, we also observed an unconformity between shale, sandstone, conglomerate, and fanglomerate layers with similar lithofacies types as above, and Paleogene red beds associated with rhyolites. We found that the "Kt red beds" also associated with intermediate volcanic rocks. The polymictic composition of the conglomerates at numerous locations (e.g., location nos. 16 and 20) indicates that the debris is of local origin.

Upper Cretaceous/Tertiary

We studied intramontane clastic deposits 8 km north of Nima County Town (75 km west of Qiling Co Lake) in a 2-km-thick section of distal fan delta deposits and several cycles with dolomite-bearing mud flat deposits and fluvial red beds (Fig. 10D; Gm, "Sm", St of Miall 1985). At Nima County Town, Neogene strata overlie Paleogene sediments at an angular unconformity (Fig. 10E).

Petrology and provenance

Stained thin sections of 21 typical sedimentary rock samples from location nos. 1, 3, 5, 7, 11, 13, 14, 16, 19, and 21 were used for quantitative compositional analyses on the medium sand fraction in order to characterize their provenance. We counted >300 grains with measurement intervals corresponding to the average clast diameter. Monomineralic, polycrystalline aggregates of feldspar and quartz were counted as "lithics".

Qiangtang block, Jurassic

Samples north of Amdo at location #11 classify as calcite-cemented arkosic arenites with moderately rounded clasts and a narrow compositional spectrum occupying a small area of the QFL diagram (Fig. 12A). Feldspar constituents may derive from granitoids. Lithic fragments are limited to shallow marine carbonate, hornfels, and intraformational shale, silt, and sandstone. The cement may have preserved the original contents of zircon, tourmaline, hornblende, apatite, sphene, garnet, biotite, chlorite, and epidote, hinting at granitoid and greenschist source rocks.

DNB/Lhasa block, Jurassic

The coarsest neritic deposits at location #13, which we interpret as a lower part of the Jurassic succession, are subarkosic and quartz arenites (Fig. 12A). The latter are fossil-free and contain minor amounts of sericitized feldspar, fragments of quartzite, and chert. The quartz grains frequently display pressure solution, but rarely syntaxial overgrowth, which also applies to the subarkosic arenites. Compared with the quartz arenites, the subarkosic arenites display a finer grain size and contain microcline, orthoclase, and Na-plagioclase. Accessory heavy minerals are zircon, hornblende, biotite, chlorite, sphene, and brookite. Both mineral groups indicate similar source rocks as above.

In the middle and upper levels of the Jurassic sequence, lithic arenites with varying feldspar/lithic fragment ratios are prevalent. Arkosic arenites are also present (Fig. 12A, group III). Towards the top of the sequence, there is a significant increase from 5 to 70% in large, angular feldspar grains due to the increasing denudation of granitoids. The lithic clasts form a wide

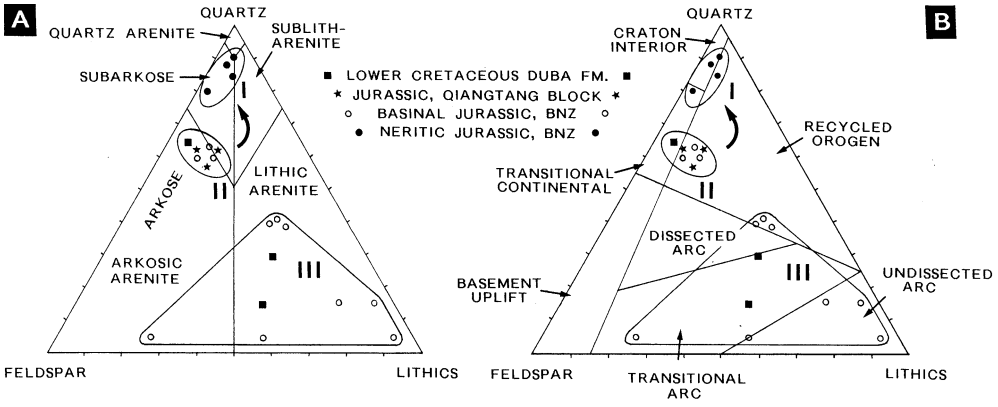

Fig. 12A, B QFL plots of Jurassic and Cretaceous sandstones of medium sand size. **A** Diagram after Pettijohn (1975). **B** Diagram after Dickinson et al. (1983). Group I: recycled sediments derived from group II. Group II: recycled sediments from the area of the Kunlun to the Qiangtang block. Group III: recycled sediments from the area of the Kunlun to the Qiangtang block and local sources

polymictic spectrum: shale, siltstone, sandstone, quartzite, calcarenite, chert, ultrabasite, basite, granitoid, and carbonate debris (e.g., location #11). The increase in carbonate grains is due to the presence of limestone olistoliths. Recrystallized shell fragments are common. Heavy minerals include zircon, hornblende, garnet, sphene, brookite, apatite, biotite, chlorite, epidote, orthopyroxene, and Cr-spinel. The latter two derive from basites and ultrabasites. The other heavy minerals stem from granitoid and greenschist sources. High-grade metamorphic minerals were not observed.

DNB/Lhasa block, Lower Cretaceous

At location #19, a type locality of the Duba Formation, lithic and arkosic arenites are prevalent (Fig. 12A) with clasts mainly from the Jurassic strata of the DNB/Lhasa block and granitoids. The heavy mineral spectrum of zircon, brookite, hornblende, apatite, epidote, biotite, and chlorite resembles that of the Qiangtang blocks' sandstones. Dravite grains (diameter 200 μm) are of pegmatitic–pneumatolytic or metamorphic origin. There is no indication for high-grade metamorphic sources.

DNB/Lhasa block, Upper Cretaceous

In the section near Duba, at location #20, the limestone content of conglomerates measures 80% (Fig. 10C). The rest is reworked Jurassic sandstone, quartzite, shale, and chert. Towards the top of the section, the limestone clasts increase in size. Lacking granitoid debris shows that the Lower Cretaceous Baingoin pluton (Fig. 13) was not yet exposed.

Main provenance trends

To trace the Jurassic and Cretaceous source areas, the contents of minerals, and the lithic fragments, the maturity, facies distribution, and transport directions are considered. Because of the similar associations of light minerals such as quartz and feldspars and heavy minerals such as zircon, tourmaline, hornblende, garnet, and epidote of the Jurassic sandstones from the Qiangtang block and DNB/Lhasa block, we conclude that the bulk of sediment was shed from the northern Kunlun/Songpan–Ganzi and the younger Songpan–Ganzi/Qiangtang accretion zones via fluvial/deltaic systems of the Qiangtang block. Harris et al. (1988a, 1988b) mentioned garnet-bearing greenschist assemblages, hornfels, and sphene-bearing granodiorites from the Kunlun. Accretion-related uplift made the Qiangtang block an effective Early Jurassic source area. Some fine-grained Jurassic components may have been shed from the southern Lhasa block into the DNB.

Granitoid and angular feldspar grains occurring in the medium and coarse sand fraction are likely of the same local origin. Paleocurrents from the east and northeast suggest the Amdo massif's granite and gneiss as additional sources. The Jurassic neritic carbonates and granitoid debris (location nos. 4, 7, and 8) show that the Amdo massif was a Jurassic structural high. The presence of sillimanite-bearing mineral associations in the Amdo massif (Harris et al. 1988a) and the lack of high-grade metamorphic detritus may or may not be a problematic aspect.

The Baingoin pluton consists of tonalite, tourmaline granite, and tourmaline–muscovite pegmatites (Harris et al. 1988b). It is too young to be a Jurassic source. We also rule it out as a source for the Duba Formation because our samples lack tourmaline, even at locations #19 and #20 near the pluton. Granitoid and hornfels debris led Leeder et al. (1988) to consider the pluton a source for the Duba Formation. We suggest that the clasts derived from the Amdo massif or a presently buried rock.

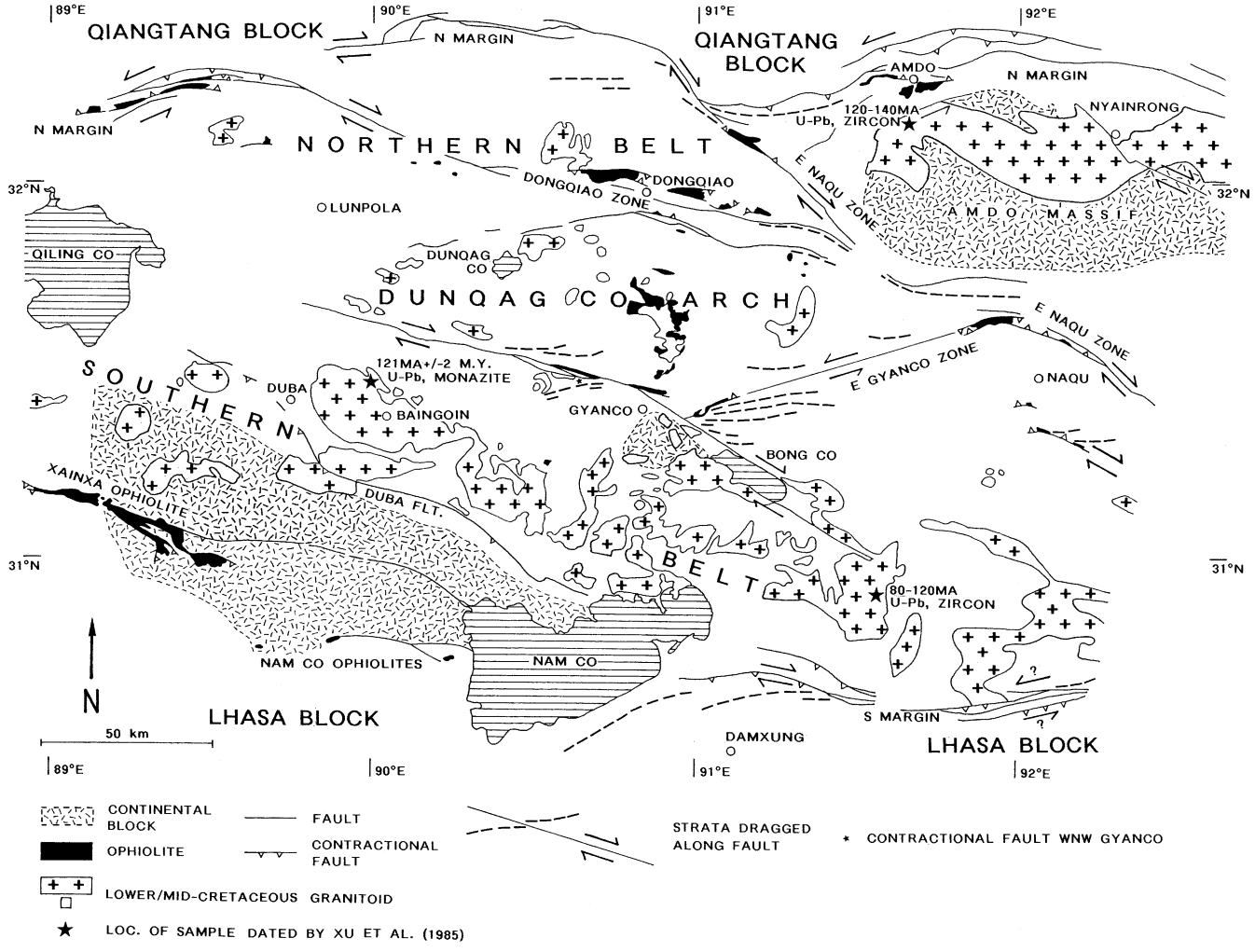

Fig. 13 Distribution of Lower/Mid-Cretaceous granitoids (simplified after Kidd et al. 1988) and the DNB's transpressional/strike-slip fault system. Elongate ophiolites appear at the faults largely bypassing continental blocks (simplified and interpreted after Kidd et al. 1988)

In the QFL diagram, Jurassic shallow marine clastics of the DNB/Lhasa block plot in the adjacent "craton interior" and "recycled orogen" fields (Fig. 12B, group I), suggesting a northern source area (Kunlun orogen to Qiangtang block) whose Mesozoic deposits have the "recycled orogen" status. Clastics of the Qiangtang block and some of the DNB/Lhasa block plot in the "transitional continental" and "recycled orogen" fields (Fig. 12B, group II), suggesting the same sources. The bulk of the Jurassic basin clastics coincides with different arc regions (Fig. 12B, group III).

Mature quartz arenites at location #13, 100 km south of the Qiangtang block (after shortening), represent reworked products of siliciclastic sediments from the Qiangtang or Lhasa blocks.

Tectofacies, depositional system, and paleogeography

Jurassic

The paleogeographic sketch (Fig. 7) illustrates the tectofacial situation for the Middle to Upper Jurassic of both the southern Qiangtang block and the DNB/Lhasa block.

The Qiangtang block's Jurassic sedimentary development reflects regional tectonism. Following Early Jurassic accretion-related uplift of this block, debris of the newly formed northern mountain range accumulated to the south as the Qiangtang block's paralic molasse wedge, which recorded a slope from the terrestrial north to the southern sea. The relative maturity of sandstones is surprising considering the short N–S transport and distinct paleoslope. Apparently, the fluvial/floodplain/deltaic system that passed into the coastal plains and sabkhas allowed for considerable reworking.

Along and across the DNB, lateral facies changes were controlled by structural highs and syndepositional ophiolite emplacement, allowing for shallow marine and terrestrial conditions. Seamounts (Pearce and Deng 1988) and oceanic arc slopes (compare Leeder et al. 1988) also may have existed. Mid- and Late Jurassic ophiolite thrusting (below) caused at least two intra-Jurassic unconformities. The olistostromes and olistoliths from the Qiangtang block indicate a steep northern basin slope along which syndepositional tectonism and seismicity may have triggered such flows. In the southern and northern part of the DNB, shallow and deep marine deposits are more common.

The DNB's sediments derived from the northeast and east, as indicated by paleocurrent directions, olistoliths, and our provenance studies and identify the northern accretion zones and the Amdo massif as source areas. The scarcity of flute casts precludes extensive paleocurrent studies. The reason seems to be low-energy sedimentation from low-density suspensions. The lack of coarse high-concentration turbidity current deposits and channel features points to the absence or scarcity of submarine fan or ramp systems. We interpret the northern basin slope as a steep, mud-rich slope apron, sensu Reading and Richards (1994). The slope was well-supplied with fine-grained material, and slumps were triggered that evolved into olistostromes, which traveled as far as Gyanco into the basin, i.e., 100 km after shortening. The southern basin margin appears to have been a neritic platform (Smith and Xu 1988; Yin et al. 1988), obviously reflecting a more gentle slope than the northern; thus, giving the basin an asymmetric shape. Due to the basin's rugged morphology, lateral facies changes, and deep and shallow marine as well as subaerial conditions existed.

Cretaceous/Tertiary

Leeder et al. (1988) interpreted the Early Cretaceous fluvial red beds as molasse derived from the north and included the Qiangtang block's Jurassic molasse. The southward progradation of the Cretaceous clastics was associated with floodplain and fluvio-distributary channel systems, but was halted by the Aptian–Albian transgression (Leeder et al. 1988). Following the marine interval, similar conditions existed as before (Dürr 1996). The immature red beds represent intramontane alluvial fans and terrestrial fan deltas whose composition is of local origin. During the Mid-Cretaceous, the Lhasa block was partly eroded and the detritus was shed southward into the Xigaze forearc basin, which formed in response to north-directed B-subduction during India's approach (Dürr 1996). At the same time, southern and central Tibet was affected by magmatism (Schärer et al. 1984; Gariépy et al. 1985; Coulon et al. 1986; Harris et al. 1988b, 1988c). The intramontane Cenozoic sediments preferably occur in E–W-trending sub-basins, displaying angular unconformities.

Definition of the BNZ

Because of the contrasting Jurassic facies, the Qiangtang block/BNZ boundary is readily defined. Also, the BNZ's northernmost ophiolites define its minimum extent to the north. Moreover, faults mark the BNZ's northern limit. The southern boundary is viewed differently. Burg et al. (1983) depicted the Lhasa block's northern limit as 120 km north of Lhasa, which corresponds to the occurrences of the Xainxa/Nam Co Lake ophiolites (Fig. 13). However, Girardeau et al. (1985) depicted the northern boundary as a suture near Amdo and north of the Qiling Co Lake, and interpreted the Xainxa ophiolite as a klippe that had been thrust for over 100 km from the suture. The reasons for this confusion are the scattered distribution of ophiolites from N–S over 150 km and the fact that "continental units" such as the Amdo massif occur between the ophiolites (Fig. 13). The presence of other "continental units" is indicated by Late Paleozoic and Mesozoic shelf deposits, which suggest there is continental basement in their subsurface (e.g., area NW of Nam Co Lake; Fig. 13). Figure 7 may aid in understanding that the DNB had a complex geometry due to the presence of continental blocks.

For the study area, we define the BNZ's northern limit by the Qiangtang block's southern margin, and the southern limit by the Nam Co Lake ophiolites (west) and the boundary between Paleozoic and Meso-Cenozoic deposits (east; area east of Nam Co Lake; Figs. 2 and 13). The following aspects support our definition by showing that the BNZ is its own unique geologic entity.

1. The BNZ's heterogeneity with alternating ophiolites and "continental units" is not typical of the adjacent continental blocks.
2. Structural observations indicate the presence of ophiolites in the subsurface allowing us to interpret the DNB as a post-Late Jurassic remnant basin (below).
3. The suggested BNZ's boundaries are mostly mapped as faults (Kidd et al. 1988).
4. The BNZ's southern limit coincides with a vertical Moho step, at the order of 20 km, with the Moho being lowered on the side of the BNZ (Hirn et al. 1984). Hirn et al. (1984) attributed this step to postsuture strike-slip. In this regard it is worth recalling that sutures often facilitate postsuture strike-slip (e.g., Sengör 1981b).
5. The partly oceanic BNZ of the study area is a Neogene/Quaternary dextral strike-slip zone of en échelon faults that traverse the BNZ, but do not enter the continental Qiangtang or Lhasa blocks (Fig. 1; Pêcher 1991), reflecting the change of material properties at the BNZ's margins.

Crustal structure of the BNZ

The seismic traverse of Hirn et al. (1984) traced the Moho at the BNZ's southern margin at a depth of 55 km. Northward, the Moho gradually shallows with the shallowest area (40 km) near Dunqag Co Lake. From there to the north, the Moho is north-dipping. Close to the Dongqiao ophiolites it was encountered at a depth of 60 km, where another vertical step with an abrupt Moho elevation of 20 km exists (Hirn et al. 1984). This step coincides with the Dongqiao fault zone.

These data show that the center of the study area represents an asymmetric arch cresting at Dunqag Co Lake. The geology reflects this structure because the crest area coincides with outcrops of Early to Mid-Cretaceous granitoids of the post-collision type (Xu et al. 1985; Kidd et al. 1988). Because they form an E–W belt, they may provide a clue as to the shape of the fault-bound arch (Fig. 13). These granitoids are generally more common along the BNZ's margins (Fig. 13).

Except for the crest of the Dunqag Co arch, ophiolite bodies occur in a straight, linear style associated with straight or gently curved contractional faults. These "ophiolite lines" trend either WNW or ENE. Other rock units may also follow this pattern.

Cretaceous sedimentary rocks also have a linear distribution tendency, often parallel to "ophiolite lines". Paleogene deposits display a straight, linear E–W distribution pattern. They are commonly found along prominent fault zones and also occur along segments of "ophiolite lines".

Girardeau et al. (1984) and Chang et al. (1989) distinguished two intervals of thrusting and folding. During the first, Jurassic deposits were thrust and folded and ophiolites were emplaced. The second included Aptian–Albian strata. Coward et al. (1988) also recognized these events and considered the latter to be of post-Mid-Cretaceous, pre-Tertiary age, producing upright to north-verging folds in the Lhasa region. In addition, they also recognized a Tertiary deformation interval, which probably reworked Mesozoic structures (Coward et al. 1988). Due to India's indentation, Tibet is subjected to a N–S compression causing E–W-oriented compressive structures (Coward et al. 1988), an E–W extension as indicated by young N–S-oriented normal faults (Tapponier et al. 1981; Armijo et al. 1986), strike-slip in a conjugate fault system (Rothery and Drury 1984), and a system of differently oriented lateral escape faults (Avouac and Tapponier 1993). Ratschbacher et al. (1991) found that folds and thrusts caused by the India/Asia collision, affecting the Eocene and possibly Oligocene to Miocene sediments, developed coevally with, but mainly predate, extension and strike-slip.

Shortening of the DNB

Mesozoic

Conventional, nontranspressional shortening is generally explained by the convergence between the Lhasa and Qiangtang blocks. The coincidence of Upper Jurassic paleosols atop thrust ophiolites west of Dongqiao (above) suggests a Late Jurassic ophiolite obduction. NW of Dongqiao, ophiolite obduction had already occurred during the early Mid-Jurassic, as indicated by the radiometric hornblende age of 179 Ma (Chang et al. 1989; method not mentioned), because the mineral formed in amphibolite at a contact aureole at the base of a hot-obducted ophiolite body (Girardeau et al. 1984).

Mid-Jurassic thrusting affected the Amdo massif where biotite-grade shear zones and later brittle thrusts accommodated tectonic transport towards the south (Coward et al. 1988). Gneiss from the massif yields a Mid-Jurassic lower intercept age for sphene of 171±6 Ma (Xu et al. 1985), which dates the regional low-grade metamorphism event linked to Jurassic shortening (Chang et al. 1989).

A large ophiolite thrust sheet must have existed south of Dongqiao, where Coward et al. (1988) observed its outliers, thrust to the SSE over Jurassic marine deposits. In the area of the Dunqag Co arch, Coward et al. (1988) carried out detailed mapping work on granitoid-intruded ophiolites of the same thrust sheet. There, Jurassic flysch was thrust over the ophiolite sheet, which, in turn, was locally thrust over Cretaceous deposits (Coward et al. 1988).

The ophiolites have generally been thrust to the south, and south-verging folds and thrusts also exist in Jurassic and pre-Jurassic sediments of the Naqu area (Coward et al. 1988). Northwest of Gyanco, they observed SE-verging structures whereas, SE of Gyanco, they noticed opposite vergence.

Coward et al. (1988) addressed some of the problems concerning the "collision" between the Lhasa and Qiangtang blocks. They observed the lack of major deformation at the present outcrop level, little evidence for crustal thickening, no evidence for the creation of a mountain belt, absence of thick molasse deposits, and, instead, the presence of widespread shallow marine Lower Cretaceous sediments. They also addressed the problem of scattered ophiolite distribution, especially that of the Xainxa/Nam Co Lake ophiolites so far south of the Qiangtang block. Taking some postemplacement shortening into account, they calculated a south-directed horizontal transport, possibly on the order of 200 km. Stating that it is unknown how the ophiolites were obducted into their present position, these workers pointed out that, if the ophiolites were emplaced by a single thrust sheet, this was probably rather thin making it difficult to imagine an adequate driving mechanism to transport this unit so far without being entirely broken. They also rejected the consideration of several sutures as an alternative because corresponding structural evidence

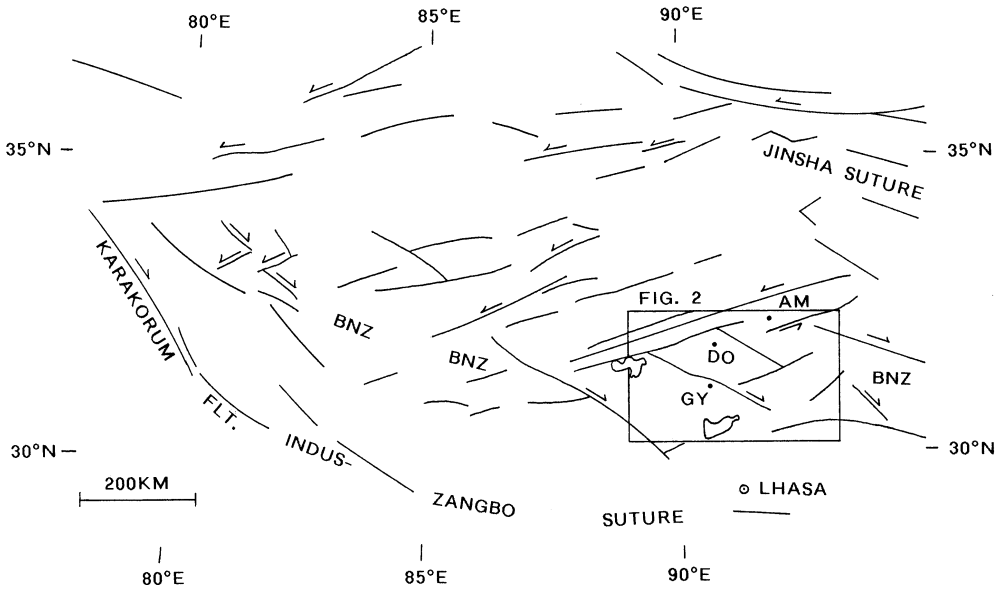

Fig. 14 Conjugate, neotectonic pure shear strike-slip fault system of dextral WNW and sinistral ENE faults accommodating India's indentation (after Rothery and Drury 1984)

and metamorphism are absent. They finally opted for an imbricated thrust sheet.[1] This option implies a thick thrust mass allowing for long distance ophiolite thrusting. The problem with this interpretation may be the lack of a corresponding degree of thrust deformation. Moreover, if one imagines a thick thrust mass consisting of obducted oceanic basement and cover rocks, ophiolite clasts should be very common in clastic post-Jurassic sediments. This, however, is not the case.

Previously, Girardeau et al. (1985) had interpreted the Xainxa ophiolite as a klippe thrust southward for 200 km because the Xainxa and Dongqiao ophiolites have "similar lithologies and tectonics". Their view, however, is incompatible with the finding of Pearce and Deng (1988), as far as the compositional aspect is concerned, in which the Xainxa ophiolites resemble forearc lithosphere and the Dongqiao ophiolites resemble backarc lithosphere. According to Pearce and Deng (1988), it may be "too simplistic to construct a single ophiolite section from isolated outcrops..." and "too simplistic to assume that all fragments represent klippen from a single suture...".

Cenozoic

Cenozoic folds trend more or less E–W and tend to be more open in Neogene strata than in Paleogene strata (Kidd et al. 1988, map). The 100-km-long and 20-km-wide, E–W-trending Lunpola basin is a main Cenozoic compressive structure. It may be described as a "compressive graben" because this elongate basin is bounded by compressive faults along its margins where the Paleo-Neogene fill was overridden, which is evidence of Neogene/Post-Neogene shortening. Yin and Harrison (2000) assumed 200 km or more of mainly Mid-Tertiary thrusting between the Lhasa and Qiangtang blocks in west Tibet. Age constraints regarding the regional Cenozoic shortening have been provided by Harrison et al. (2000), who distinguished two episodes of shortening close to the Zangbo suture: one between 30 and 23 Ma, and one between 25 and 10 Ma.

Strike-slip tectonics

The study area is traversed by a Miocene to present dextral simple shear zone (Fig. 1) with left-stepping, en échelon, WNW-trending lateral escape faults (Armijo et al. 1983; Pêcher 1991), and, at the same time, it is part of a neotectonic pure shear strike-slip system of dextral WNW and sinistral ENE faults accommodating India's indentation (Fig. 14; Rothery and Drury 1984). Both systems coincide in their dextral faults.

Transpression is more important than previously noticed in explaining the linear ophiolite distribution. In general, obducted ophiolites are associated with contractional faults. In the study area, however, the associated contractional faults or fault belts are strikingly straight to gently curved. Map analysis shows that faults other than low angle thrusts control this pattern. We suggest that it is caused by transpression based on (1) consideration of the straightness of strike-slip faults and related geomorphic features, (2) shear sense indicators, (3) coupled shear pattern/subsidence analyses (e.g., pull-aparts), (4) consideration of established examples of strike-slip zones, and (5) the interpretation of the map by Kidd et al. (1988), referred to below as "map" or "mapped".

The BNZ's northern margin displays a sinuous shape (Fig. 13). The shear sense depends on the fault's regional trend: dextral at WNW and E–W segments and sinistral at

[1] In western Tibet where the ophiolite distribution is less wide (approximately 70 km N–S extent) than in the DNB, Kapp (2001) and Kapp et al. (2003) interpreted the ophiolite distribution in terms of a thrust-faulted north-dipping subduction-accretion complex.

ENE segments. North of Qiling Co Lake, the BNZ and Qiangtang blocks' Jurassic are fault-separated (Kidd et al. 1988), and several contractional (transpressional?) faults that trending 70° are associated with elongate ophiolites. Towards the east, the northern margin fault trends 90°, and Jurassic, Paleogene, and Neogene deposits are right-laterally displaced. The Paleogene and Neogene strata may have sealed the block margin first before dextral separation occurred/recurred. The map also indicates orientations of folds in these strata, consistent with the asymmetry of a sinistral shear zone (see Harding 1974).

Farther east (40 km N Dongqiao), Neogene beds cover the northern margin fault, but the proximity of the BNZ and Qiangtang blocks' different Jurassic strata allow us to narrow down the position of the fault. The geomorphology and Jurassic outcrops indicate a SE fault trend. Farther southeast, the northern margin fault is mapped between the two different Jurassic rocks, trending 135°. Here the marginal shear zone splits into two branches. One continues with a trend of 135°, which is approximately parallel to the dextral fault direction, and enters the BNZ as the "E Naqu zone". The other takes an overall ENE trend as the northern margin fault. The map shape of the ophiolite body located at the fault junction reflects the branching of the fault (Fig. 13). The ophiolite is bound by a contractional fault (Kidd et al. 1988) and occurs in a zone of dextral transpression (He et al. 1991).

The eastward continuation of the BNZ's northern margin trends ENE in the Amdo region, where two elongate ophiolite bodies occur (Fig. 13) within a sinistral transpression belt displaying bipolar, outward-directed thrusts to the north and south, which are reminiscent of positive flower structures (Coward et al. 1988; Kidd et al. 1988, their Fig. 4). The sinistral shear sense was determined by offset markers and slickenside analysis (Coward et al. 1988; Kidd et al. 1988). Supporting this evidence, we add that the geometric relation between the bipolar thrusts and the belt's trend suggests sinistral slip (see Harding 1974). Ophiolites, "Kt red beds," and andesites take part in the deformation (Kidd et al. 1988). According to Pearce and Mei (1988), the volcanic rocks of this section have been dated by Coulon et al. (1986) as Campanian. Biotite from andesite yields a well-defined ^{39}Ar–^{40}Ar age plateau at 76.6±1.5 Ma, and a Rb–Sr whole-rock (feldspar, biotite) isochron age of 80.5±1.4 Ma was obtained for dacite (Coulon et al. 1986). A small amount of this sinistral transpressional deformation occurred during the Quaternary (Kidd and Molnar 1988; Kidd et al. 1988).

Farther east, the map shows no shear sense indicators for the northern margin fault. To the south of the fault, where it trends ESE, at Nyainrong, a dextral fault parallels the margin, displacing Lower Cretaceous (Xu et al. 1985) granitoid and metamorphic rocks of the Amdo massif (Fig. 2).

The E Naqu zone belongs to the dextral fault set. Its central segment intersects with "Kt rocks," which are dextrally dragged (Fig. 13). He et al. (1991) interpreted the northern and central segments of the E Naqu zone as a Late Jurassic to Early Cretaceous dextral transpression zone. North of Naqu, the fault is marked by a small elongate ophiolite body and a long, narrow Paleozoic sedimentary rock unit, both bound by contractional SE-trending faults (Fig. 13). A large elongate ophiolite unit extending from the southerly located E Gyanco zone into the E Naqu zone is also dextrally dragged (Fig. 13). It is bound by contractional (transpressional?) faults. South of Naqu, two small elongate ophiolite units parallel the E Naqu zone, bound by a contractional (transpressional?) WNW-trending fault along which "KT beds" are dextrally dragged (Fig. 13).

The Gyanco/Bong Co Lake zone belongs to the dextral fault set. At Gyanco, the fault trend changes from 105° in the west to 125° in the east (Fig. 13). In the west, two linear ophiolite units and a seemingly narrow dextral pull-apart sag with Quaternary (and older?) fill occur. For the Gyanco area, Coward et al. (1988) has identified WNW-trending dextral Neogene faults. At the western end, Paleogene deposits may have first sealed the fault before shearing occurred/recurred. On both sides of the western segment, Jurassic sediments were dextrally dragged. The orientation of a fold in these Jurassic rocks suggests dextral slip (see Harding 1974). The eastern segment consists of two presently active, right-stepping dextral faults, forming the Bong Co Lake pull-apart basin (Fig. 13; Armijo et al. 1983). North of this fault segment, "Kt strata" exhibit dextral drag and a granite is dextrally displaced along the pull-apart basin (Fig. 13).

The E Gyanco zone is part of the sinistral fault set (Fig. 14). Two elongate ophiolites associated with contractional (transpressional?) faults occur in this fault, which is marked by a straight valley. Jurassic and "Kt beds" on the northern and southern sides display sinistral drag (Fig. 13).

The Dongqiao zone is part of the dextral fault set. It is marked by numerous ophiolites (Fig. 13) associated with contractional (transpressional?) faults and a Moho step due to postsuture strike-slip (Hirn et al. 1984). Eastward, the fault joins the east Naqu zone, and to the west it joins the northern margin fault as revealed by short segments of mapped faults and geomorphology (straight narrow valley), suggesting that the Dongqiao zone is mechanically linked to and part of the fault system.

The southern margin zone of the BNZ is complex. Because its trend varies, the shear sense may vary (Fig. 13). In the east, the southern margin is well defined because the BNZ's Mesozoic strata are in fault contact with the Lhasa block's Paleozoic rocks. The contact occurs in a zone of straight, parallel, closely spaced faults that includes contractional (transpressional?) faults. This segment lacks map-scale shear sense indicators. Its trend suggests that it belongs to the sinistral set.

To the west, north of Damxung, the trend changes. Paleozoic rocks exhibit dextral drag and the fault zone splits up into two strands (Fig. 13). Under Nam Co Lake, one of the two may split again. The northern branch continues WNW of the lake as the Duba fault, along which a contractional (transpressional?) contact between

the Paleogene and Cretaceous strata exists (Leeder et al. 1988). The central branch fault connects with the elongate, 75-km-long Xainxa ophiolite (Fig. 13), which is associated with contractional (transpressional?) faults. At the segment near Nam Co Lake, Coward et al. (1988) noticed a "zone of probably steep strike-slip Neogene faults". The third branch may link up with the Nam Co ophiolites, which coincide with a postsuture strike-slip Moho step (Hirn et al. 1984). The trend of the three branch faults suggests that they are part of the dextral fault set.

Shallow marine Late Paleozoic and Mesozoic rocks of the southern BNZ and northern Lhasa block (Leeder et al. 1988; Smith and Xu 1988; Yin et al. 1988) signal the presence of continental crust in the subsurface north of the Xainxa and Nam Co ophiolites. We suggest that these continental units of the DNB were once surrounded by oceanic crust, and that the ophiolites have their roots in faults now separating the continental units. From these faults they were thrust for only up to 10 km to the south. If one interprets these continental units as the Lhasa block's northern limit, a thrust range of 75 km would have to be considered.

Significance and time constraints of strike-slip movements

The abundant coincidence of linear ophiolite bodies, contractional faults, drag effects, documented strike-slip, and the presence of two established transpression belts suggests that many ophiolites were squeezed up by transpression from the local subsurface with only minor thrust ranges. The abundance of ophiolites in the shear zones suggests the relatively widespread presence of oceanic basin floor in the subsurface. The DNB's heterogeneous crust consists of oceanic and continental domains. Due to lesser shear strength, the movements preferably occurred in oceanic domains leaving continental blocks largely unaffected. Our concept rivals an explanation of the "ophiolite lines" due to conventional thrusting. It eliminates the call for a difficult to justify thrust mass once covering the study area and related long-range ophiolite thrusting.

Post-Campanian and Quaternary strike-slip is evident. Earlier movements appear possible. In the Amdo transpression belt, deformed Campanian volcanic rocks time-constrain deformation. Late Cretaceous activity could correlate with the post-Mid-Cretaceous, pre-Tertiary deformation interval of Coward et al. (1988). Paleogene strata may have sealed two faults before they were sheared. During the Neogene to Quaternary, some faults were reactivated left- or right-laterally depending on their orientation. If some strike-slip had occurred during the Late Cretaceous, the Cretaceous depositional change from marine to terrestrial may have been due to transpression-related uplift. Late Jurassic to Early Cretaceous movements appear possible to some authors (He et al. 1991).

Cenozoic extension

The study area's normal faults are N–S oriented. Grabens are often marked by lakes (Fig. 2). The grabens' length and width may measure up to 50 and 15 km, respectively. There are also half grabens such as the relatively large one SE of Xiongmei (Fig. 2).

Extension of the Tibet plateau may have started before 13.5 Ma (Blisniuk et al. 2001), ~14 Ma (Coleman and Hodges 1995), 11–10 Ma (Garzione et al. 2000), or 13.3±0.8 Ma (Williams et al. 2001). For the study area, extension during the Quaternary including historic times is documented (Tapponier et al. 1981; Armijo et al. 1986).

Basin evolution

Because the rift flank sequences indicate transtensional basin formation (Mattern et al. 1998) and because transpression played a major role in the destruction of the oceanic basin floor, the DNB's evolution represents a Reading cycle (see Introduction; Reading 1980; Mitchell and Reading 1989) despite tectonic events unique to the DNB's cycle.

The Permian to Late Triassic represents the stage of transtensional basin formation. The initial setting was a backarc (Fig. 15). Permian volcanism of the Lhasa and Qiangtang blocks is of backarc or extensional rift affinities (Leeder et al. 1988). The composition of the 1.5-km-thick Late Carboniferous or Permian (Smith and Xu 1988) Dagze volcanic rocks east of Lhasa, and the Triassic volcanic rocks located 50 km NW of Lhasa, reflect volcanic arc activity on transitional crust (Pearce and Mei 1988). The positions of arc and backarc imply north-dipping B-subduction. While the DNB opened, also southward B-subduction occurred north of the Qiangtang block consuming the Paleo-Tethys Ocean (Fig. 15; Dewey et al. 1988; Mattern and Schneider 2000). The volcanic rocks of the early Late Triassic Batang Group (Smith and Xu 1988) of the northern Qiangtang block represent the corresponding magmatic arc (Pearce and Mei 1988). The backarc interpretation is also supported by geochemical ophiolite studies (Göpel et al. 1982; Girardeau et al. 1985).

At active margins, there is a higher probability of oblique than head-on convergence. The former commonly causes trench-linked strike-slip faults in the upper plate (Woodcock 1986). Thus, due to the presence of two B-subduction zones, strike-slip in the upper plate appears especially likely to have occurred, leading to transtensional rifting of the carbonate platform and formation of the DNB. According to Yu et al. (1991), the northern margin of the BNZ displays an s-shape in map view (Fig. 1), which implies a sinistral shear sense.

Spreading created a relatively wide oceanic backarc basin. This is implied by our conclusion that the continental blocks of DNB were surrounded by oceanic crust and by the existence of forearc and backarc lithosphere in the DNB (Pearce and Mei 1988). We thus

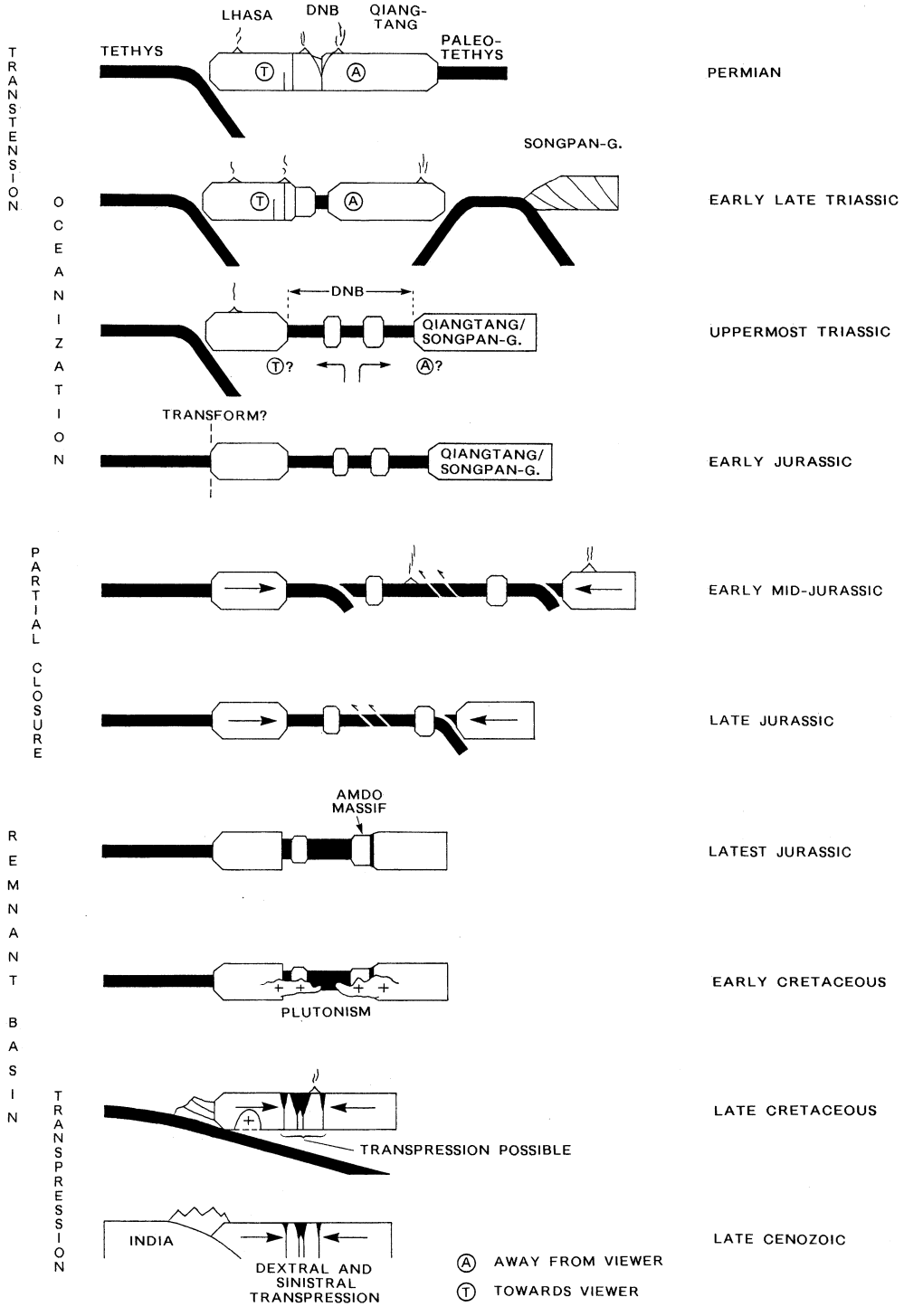

Fig. 15 Plate tectonic development of the DNB. There may have been more than two continental blocks within the oceanic DNB. The amount of the DNB's subducted ocean floor may have been small. Post-Jurassic thrust structures are omitted

consider oblique spreading a more likely spreading mechanism than pure pull-apart which was important during rifting.

The basin was oceanized during the Late Triassic to Early Jurassic. The preflysch rocks are either basaltic or terrestrial, as in the Naqu area from where Yin et al. (1988, pullout 1) described the >2-km-thick clastic, coal-bearing Late Triassic Tumaingela Formation. The basin was below sea level at the Triassic/Jurassic boundary. Pillow lavas may occur in the Jurassic flysch (location #21).

During the Jurassic, the Lake Area Flysch and chert were deposited in deep basinal positions whereas shallow marine carbonate accumulated at structural highs (e.g., Lunpola area). Olistostromatic deposition was significant at the northern basin slope (Fig. 7).

Because an Early Jurassic arc is absent, subduction and the DNB's backarc history must have ended close to the

Triassic/Jurassic boundary. If transtension did continue, a transform mechanism would have to be considered. In the south, where no indication for a Late Triassic/Early Jurassic accretion event exists, subduction may have been replaced by transform motion. In the north, subduction ceased due to closure of the Paleo-Tethys Ocean and accretion of the Qiangtang block onto the Songpan Ganzi belt. Continued convergence in this sector may have affected the DNB during the early Mid- to Late Jurassic, causing an episode of partial basin closure as indicated by ophiolite thrusting (Fig. 15). Basin shortening may have caused shallowing of the marine environment, especially above emplaced ophiolites. Otherwise, the depositional pattern remained similar to before.

According to Allègre et al. (1984), the DNB was consumed during the Late Mesozoic by a north-dipping B-subduction zone north of the Lhasa block with the arc located on oceanic crust of the DNB. The model for the Jurassic by Pearce and Deng (1988) is similar and includes oblique backarc spreading with a sinistral component. The arc is represented by Jurassic volcanic rocks north and SW of the Amdo massif (Pearce and Mei 1988; Pearce and Deng 1988). This model accounts for the zonation of rock types such as forearc ophiolites, volcanic arc rocks, and backarc amphibolites from south to north. Pearce and Deng (1988) found evidence of seamount edifices. Their model of a tectonically active basin with a rugged morphology is helpful in explaining the frequent occurrence of gravity mass flow deposits (e.g., olistostromes) and lateral facies changes.

Whether the Qiangtang block was affected by arc magmatism is unclear. The characteristics of early Mid-Jurassic basic volcanic rocks of the Yanshiping Group (Smith and Xu 1988), north of Wenquan, are ambiguous (Pearce and Mei 1988). Igneous rocks to the north of the BNZ are scarce (Allègre et al. 1984; Dewey et al. 1988), and Dewey et al. (1988) concluded that "subduction was so slow ... that no magmatism was produced."

We characterize the Late Jurassic to Early Cretaceous as a remnant basin stage. Despite the basin's partial closure during the Mid–Late Jurassic, parts of the basin floor and Jurassic fill have been preserved in the study area (Fig. 15). The lack of a major (e.g., basin-wide) depositional change from marine to terrestrial conditions following ophiolite obduction is consistent with the remnant basin concept. The BNZ's wide outcrop zone can be partly attributed to the presence of continental blocks that acted as rigid objects during basin shortening. It can also be explained in terms of a remnant basin whose opposite margins "do not fit." The conclusion that the eastern BNZ is underlain by much ophiolite is also consistent with the remnant basin concept. In agreement are also structural indications, as provided by Coward et al. (1988), who noticed that little deformation was associated with the "collision" between the Qiangtang and Lhasa blocks and that there is little evidence for major crustal thickening of the Qiangtang block whose Mesozoic sediments are only weakly deformed. They also realized that, across the Lhasa block, there is no evidence for a Late Mesozoic mountain belt and related thick molasse deposits. Instead Aptian–Albian limestone extends across the area, suggesting shallow marine conditions. Similarly, Dewey et al. (1988) noticed the lack of significant deformation at the time of the "collision".

Deposition of thick Jurassic flysch continued in deeper parts of the basin, and shallow marine deposition continued on structural highs. Cooling and subsiding remnant oceanic basin floor would allow for deep marine conditions and the deposition of the DNB's Late Jurassic chert.

In the BNZ, a bimodal suite of metaluminous tonalite–granodiorite and two-mica granites occurs (Harris et al. 1988b), which were emplaced around 140 to 80 Ma (Figs. 13 and 15) in a post-collision setting (Xu et al. 1985; Harris et al. 1988b). Plutonism began approximately with a change from marine to terrestrial deposition and ended with a recurrence of marine conditions during the Aptian–Albian. These changes are consistent with global eustatic sea-level changes (see Haq et al. 1988). If, however, a relation with magmatic activity should exist, thermal doming could be causally considered for the terrestrial episode and cooling-related subsidence of the dome corresponding to waning magmatism for the marine interval.

While continuing to be a remnant basin, the DNB became a backarc basin again during the Early Cretaceous to Mid-Eocene. The marine depositional interval occurred in a backarc setting. According to Coulon et al. (1986), the composition of certain Cretaceous and Paleogene volcanic rocks of southern and central Tibet has arc properties. Based on their ^{39}Ar–^{40}Ar ages and literature data they showed that the ages range between 110 and 80 Ma in the north and between 60 and 50 Ma in the south, which they attributed to India's approach from the south and the related N-directed subduction of oceanic lithosphere from 120 to 40 Ma with shallow subduction until 80 Ma, followed by steeper subduction. The plutonic Gangdese belt of the southern part of the Lhasa block is a manifestation of this subduction zone (Schärer et al 1984; Gariépy et al. 1985; Harris et al. 1988b, 1988c). While sedimentation was coeval with subduction, the DNB was a remnant as well as a backarc basin. After cessation of marine conditions, terrestrial red beds were deposited. This basin stage may overlap with the transpressional basin stage. Recently, Roger et al. (2000) discussed whether Eocene magmatites of the Qiangtang block formed due to renewed subduction from the Jinsha suture or BNZ.

Following the Mid-Cretaceous, the DNB went through a transpressional basin cycle. Transpression is attributed to N–S confinement, which explains the geometry of the observed shear pattern and is compatible with India's drift (Fig. 15). Confining strike-slip exhumed ophiolites from the local subsurface in linear belts (Figs. 13 and 15). Cretaceous magmatism reduced the DNB's shear strength making it more susceptible to this deformation. N–S confinement may also have had some control in forming E–W-trending intramontane sub-basins. As of the Mid-

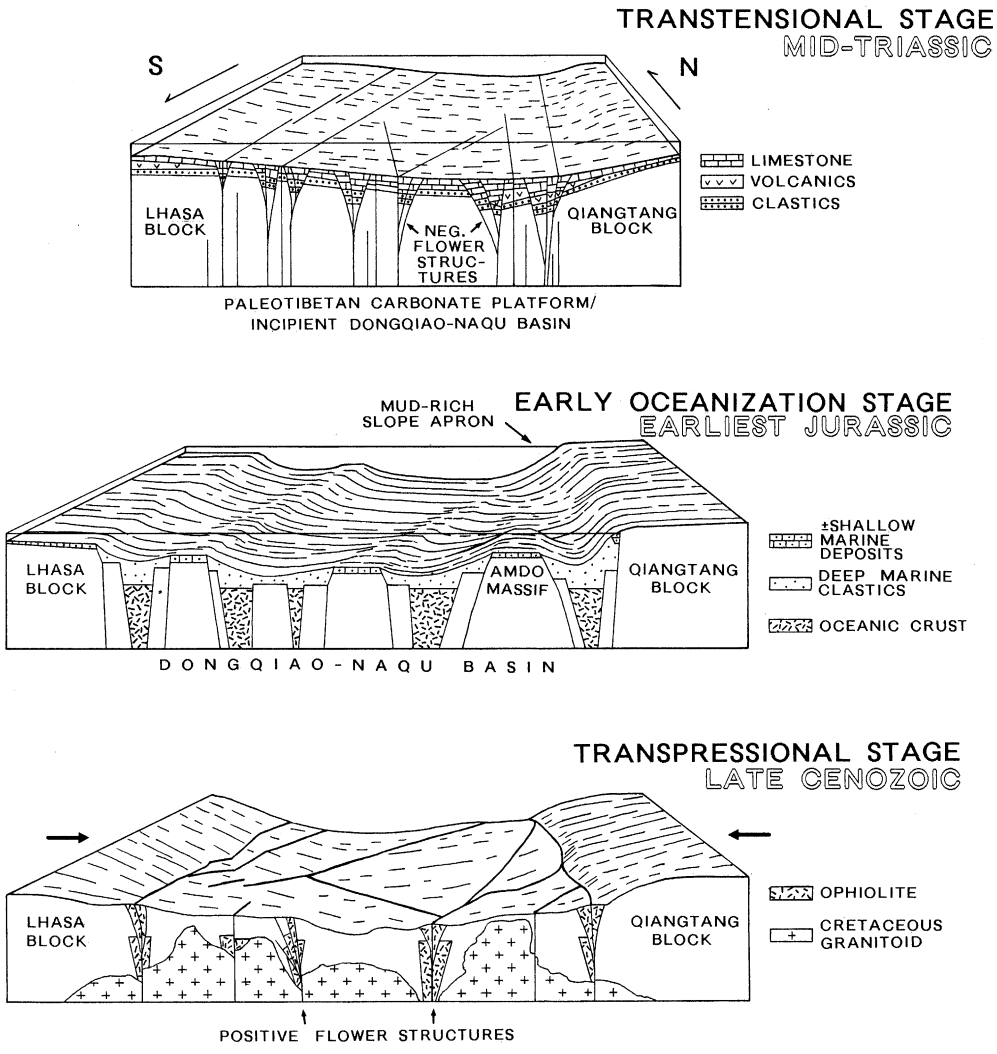

Fig. 16 Evolutionary stages of the DNB, consistent with a Reading cycle (not to scale). Whether the Amdo massif was completely submerged during the earliest Jurassic is uncertain

Cretaceous, deposition is terrestrial leading to the accumulation of alluvial fans, fan deltas, and lacustrine deposits.

Transpression possibly occurred during the Cenomanian, causing uplift and termination of marine conditions. It may correlate with the post-Mid-Cretaceous, pre-Tertiary deformational interval of Coward et al. (1988), or with folding of Cretaceous strata, which, according to Achache and Courtillot (1984), occurred between 80 and 60 Ma (Campanian–Paleocene). They related folding to confining active margin tectonics that resulted from a colliding oceanic plateau, or seamount province, or aseismic ridge generated by the Réunion hot spot. Coulon et al. (1986) restricted folding of the same rocks to between 110 and 90 Ma (Albian–Turonian), attributing it to shallow subduction and tight plate coupling resulting in a compressive backarc. Accretionary wedge formation as of the Mid-Cretaceous south of the Lhasa block (Einsele et al. 1994) suggests a high rather than a low degree of plate coupling. In any case, compression of the backarc is related to active margin tectonics.

India's collision and indentation promoted transpression (e.g., Amdo belt) and was associated with plateau uplift (e.g., Zheng et al. 2000, and sources therein), crustal thickening (e.g., Dewey et al. 1988), lateral escape tectonics along intracontinental strike-slip faults (e.g., Avouac and Tapponier 1993), and neotectonic E–W-directed extension providing for the last imprints on the DNB with the latter causing formation of a sub-basin set of N–S-trending grabens and half grabens.

Conclusions

The DNB is a polycyclic basin. Its evolution from transtensional rifting via oceanization to transpression of the remnant basin represents a Reading cycle (Fig. 16, Reading 1980; Mitchell and Reading 1989). Our concept eliminates key difficulties in the understanding of the BNZ and simplifies regional understanding. Our model explains similar prerift sequences on the Lhasa and Qiangtang blocks. Moreover, it eliminates the need to

look for typical collisional thrust deformation, related thickening, mountain-building, and thick molasse formation. In addition, the systematic regional linear ophiolite distribution pattern within strike-slip zones and between continental units is much more suitably explained by a large system of transpression belts pressing up ophiolites from local basin floor than by conventional ophiolite thrusting and subsequent erosion. Our model also eliminates the problem of having to consider difficult to justify long-range ophiolite thrusting of a single thrust mass. Thus, the ophiolites occurring in linear belts represent parautochthonous rather than allochthonous units. Positive flower structures explain opposite thrust vergences. Our model and observations for east Tibet do not support the idea of a major amount of thrusting between the Lhasa and Qiangtang blocks. The DNB's Jurassic asymmetric configuration with a steep northern and a gentle southern slope (Yu et al. 1991) is a feature quite typical for strike-slip basins (e.g., Mitchell and Reading 1989; Ben-Avraham 1992). The basin was increasingly "continentized" by granitoid plutonism and depletion of oceanic material through transpressional shearing of oceanic basement.

Acknowledgements We thank Carmala Garzione and An Yin for their constructive review of the manuscript, Deutsche Forschungsgemeinschaft for financial support, and the Geological Survey in Lhasa for accommodation and general support.

References

Achache J, Courtillot V (1984) Paleogeographic and tectonic evolution of southern Tibet since Mid-Cretaceous time: new paleomagnetic data and synthesis. J Geophys Res 89:10311–10339

Allègre CJ, Courtillot V, Tapponier P et al. (1984) Structure and evolution of the Himalaya–Tibet orogenic belt. Nature 307:17–22

Armijo R, Tapponier P, Han T (1983) Active "en échelon" right-lateral strike-slip faults in southern Tibet. Terra Cognita 3:263

Armijo R, Tapponier P, Mercier JL, Han TL (1986) Quaternary extension in southern Tibet: field observations and tectonic implications. J Geophys Res 91:13803–13872

Avouac J-P, Tapponier P (1993) Kinematic model for active deformation in Central Asia. Geophys Res Lett 20:895–898

Bally AW, Allen CR, Geyer RB et al. (1980) Notes on the geology of Tibet and adjacent areas—report of the American plate tectonics delegation to the People's Republic of China. US Geol Surv Open File Rep 80-501, Washington, DC

Ben-Avraham Z (1992) Development of asymmetric basins along continental transform faults. Tectonophysics 215:209–220

Blisniuk PM, Hacker BR, Glodny J et al. (2001) Normal faulting in central Tibet since at least 13.5 Myr ago. Nature 412:628–632

Burg J-P, Proust F, Tapponier P, Chen GM (1983) Deformation phases and tectonic evolution of the Lhasa block (southern Tibet, China). Eclogae Geol Helv 76:643–665

Chang C, Chen N, Coward MP et al. (1986) Preliminary conclusions of the Royal Society and Academia Sinica 1985 geotraverse of Tibet. Nature 323:501–507

Chang C-F, Pan YS, Sun Y-Y (1989) The tectonic evolution of Qinghai–Tibet plateau: a review. In: Sengör AMC (ed) Tectonic evolution of the Tethyan region. NATO ASI Series C 259. Kluwer, Dordrecht, pp 415–476

Coleman M, Hodges K (1995) Evidence for Tibetan plateau uplift before 14 Myr ago from a new minimum age for east–west extension. Nature 374:49–52

Coulon C, Maluski H, Bolliger C, Wang S (1986) Mesozoic and Cenozoic volcanic rocks from central and southern Tibet: ^{39}Ar–^{40}Ar dating, petrological characteristics and geodynamical significance. Earth Planet Sci Lett 79:281–302

Coward MP, Kidd WSF, Pan Y et al. (1988) The structure of the 1985 Tibet Geotraverse, Lhasa to Golmud: Phil Trans R Soc Lond A 327:307–336

Dewey JF, Shackleton RM, Chang C, Sun Y (1988) The tectonic evolution of the Tibetan Plateau. Phil Trans R Soc Lond A 327:379–413

Dickinson WR, Beard LS, Brakenridge GR et al. (1983) Provenance of North American Phanerozoic sandstones in relation to tectonic setting. Geol Soc Am Bull 94:222–235

Dürr SB (1996) Provenance of Xigaze fore-arc basin clastic rocks (Cretaceous, south Tibet). Geol Soc Am Bull 108:669–684

Einsele G, Liu B, Dürr S et al. (1994) The Xigaze forearc basin: evolution and facies architecture (Cretaceous, Tibet). Sediment Geol 90:1–32

Füchtbauer H, Richter D (1988) Karbonatgesteine. In: Füchtbauer H (ed) Sediment–Petrologie Teil II. Sedimente und Sedimentgesteine. Schweizerbart, Stuttgart, pp 233–434

Gariépy C, Allègre CJ, Xu R-H (1985) The Pb-isotope geochemistry of granitoids from the Himalaya–Tibet collision zone: implications for crustal evolution. Earth Planet Sci Lett 74:220–234

Garzione CN, Dettman DL, Quade J et al. (2000) High times on the Tibetan Plateau: paleoelevation of the Thakkhola graben, Nepal. Geology 28:339–342

Girardeau J, Marcoux J, Allègre CJ et al. (1984) Tectonic environment and geodynamic significance of the Neo-Cimmerian Donqiao ophiolite, Bangong–Nujiang suture zone, Tibet. Nature 307:27–31

Girardeau J, Marcoux J, Fourcade E et al. (1985) Xainxa ultramafic rocks, central Tibet, China: tectonic environment and geodynamic significance. Geology 13:330–333

Göpel C, Dupré B, Allègre CJ, Xu RH (1982) Constraints on the origin of two Tibetan ophiolites from lead isotopes. EOS 63:1094

Haq BU, Hardenbol J, Vail P (1988) Mesozoic and Cenozoic chronostratigraphy and cycles of sea-level change. In: Wilgus CK, Hastings BS et al. (eds) Sea-level changes: an integrated approach. Soc Econ Paleontol Mineral Spec Publ 42:71–108

Haq BU, Van Eysinga FWB (1998) Geological time table, 5th edn. Elsevier, Amsterdam

Harding TP (1974) Petroleum traps associated with wrench faults. Am Assoc Petrol Geol Bull 58:1290–1304

Harland WB, Armstrong RL, Cox AV et al. (1990) A geologic time scale. Cambridge University Press, Cambridge

Harris NBW, Holland TJB, Tindle AG (1988a): Metamorphic rocks of the 1985 Tibet Geotraverse, Lhasa to Golmud. Phil Trans R Soc Lond A 327:203–213

Harris NBW, Xu R, Lewis CL, Jin C (1988b) Plutonic rocks of the 1985 Tibet Geotraverse, Lhasa to Golmud. Phil Trans R Soc Lond A 327:145–168

Harris NBW, Xu R, Lewis CL et al. (1988c) Isotope geochemistry of the 1985 Tibet Geotraverse, Lhasa to Golmud. Phil Trans R Soc Lond A 327:263–285

Harrison TM, Yin A, Grove N et al. (2000) The Zedong Window: a record of superposed Tertiary convergence in southeastern Tibet. J Geophys Res 105:19211–19230

He J, Liu C, Liu Z, Tan F (1991) Petrological studies from Qüxü to Amdo, Xizang. Bull Chengdu Inst Geol Miner Resour 13:64–78

Hirn A, Nercessian A, Sapin M et al. (1984): Lhasa block and bordering sutures—a continuation of a 500-km Moho traverse through Tibet. Nature 307:25–27

Hsü KJ, Guitang P, Sengör AMC et al. (1995) Tectonic evolution of the Tibetan Plateau: a working hypothesis based on the archipelago model of orogenesis. Int Geol Rev 37:473–508

Jaeger JJ, Adloff C, Doubinger J et al. (1982) The contribution of fossils to paleogeography of the Lhasa block (Tibet). EOS 63:1093

Kapp PA (2001) Tectonic evolution of the Qiangtang Terrane and the Bangong–Nujiang suture zone, central Tibet. PhD Thesis, University of California, Los Angeles

Kapp P, Yin A, Manning CE et al. (2000) Blueschist-bearing metamorphic core complexes in the Qiangtang block reveal deep crustal structure of northern Tibet. Geology 28:19–22

Kapp P, Murphy P, Yin A et al. (2003) Mesozoic and Cenozoic tectonic evolution of the Shiquanhe area of western Tibet. Tectonics (in press)

Kidd WSF, Molnar P (1988) Quaternary and active faulting observed on the 1985 Academia Sinica–Royal Society Geotraverse of Tibet. Phil Trans R Soc Lond A 327:337–363

Kidd WSF, Pan Y, Chang C et al. (1988) Geological mapping of the 1985 Chinese–British Tibetan (Xizang–Qinghai) Plateau geotraverse route. Phil Trans R Soc Lond A 327:287–305 and 1:50,000 map of traverse (enclosure)

Leeder MR, Smith AB, Yin J (1988) Sedimentology, palaeoecology and palaeoenvironmental evolution of the 1985 Lhasa to Golmud Geotraverse. Phil Trans R Soc Lond A 327:107–143

Li H (1986) Upper Jurassic (Early Tithonian) radiolarians from southern Bangong Lake, Xizang. Acta Micropal Sinica 3:297–315

Mattern F, Schneider W (2000) Suturing of the Proto- and Paleo-Tethys Oceans in the western Kunlun (Xinjiang, China). J Asian Earth Sci 18:637–650

Mattern F, Schneider W, Wang P, Li C (1998) Continental strike-slip rifts and their stratigraphic signature: application to the Bangong/Nujiang zone (Tibet) and the South Penninic zone (Alps). Geol Rundsch 87:206–224

Miall AD (1985) Architectural-element analysis: a new method of facies analysis applied to fluvial deposits. Earth-Sci Rev 22:261–308

Mitchell AHG, Reading HG (1989) Sedimentation and tectonics. In: Reading HG (ed) Sedimentary environments and facies. Blackwell, Oxford, pp 471–519

Murphy MA, Yin A, Harrison TM et al. (1997) Did the Indo-Asian collision alone create the Tibet plateau? Geology 25:719–722

Pan G, Zheng H (1983) A preliminary study on Bangong Co-Nujiang suture (in Chinese). Contrib Geol Qinghai–Xizang (Tibet) Plateau 12:229–242

Pearce JA, Deng W (1988) The ophiolites of the Tibet Geotraverse, Lhasa to Golmud (1985) and Lhasa to Katmandu (1986). Phil Trans R Soc Lond A 327:215–238

Pearce JA, Mei H (1988) Volcanic rocks of the 1985 Tibet Geotraverse: Lhasa to Golmud. Phil Trans R Soc Lond A 327:169–201

Pêcher A (1991) The contact between the higher Himalaya crystallines and the Tibetan sedimentary series: Miocene large-scale dextral shearing. Tectonics 10:587–598

Pettijohn FJ (1975) Sedimentary rocks, 3rd edn. Harper and Row, New York

Pickering KT, Hiscott RN, Hein FJ (1989) Deep marine environments. Unwin Hyman, London

Ratschbacher L, Frisch W, Chen C, Pan G (1991) Tertiary compression, extension and strike-slip faulting in Tibet and western Sichuan. Terra Abstr 3:123

Reading HG (1980) Characteristics and recognition of strike-slip fault systems. In: Ballance PF, Reading HG (eds) Sedimentation in oblique-slip mobile zones. Spec Publ Int Ass Sediment 4:7–26

Reading HG, Richards M (1994) Turbidite systems in deep-water basin margins classified by grain size and feeder system. Am Assoc Petrol Geol Bull 78:792–822

Roger F, Tapponier P, Arnoud N et al. (2000) An Eocene magmatic belt across central Tibet: mantle subduction triggered by the Indian collision? Terra Nova 12:102–108

Rothery DA, Drury S (1984) The neotectonics of the Tibetan plateau. Tectonics 3:19–26

Schärer U, Xu R-H, Allègre CJ (1984) U–Pb geochronology of the Gangdese (Transhimalaya) plutonism in the Lhasa–Xigaze region, Tibet. Earth Planet Sci Lett 68:311–320

Sengör AMC (1981a) The evolution of Paleo-Tethys in the Tibetan segment of the Alpides. In: Proc Symp Qinghai–Xizang (Tibet) Plateau (Beijing, China), geological and ecological studies of Qinghai–Xizang Plateau, vol 1. Geology, geological history and origin of Qinghai–Xizang Plateau. Science Press, Beijing and Gordon and Breach, New York, pp 51–56

Sengör AMC (1981b) Strike-slip motion along the Tethyside sutures: implications for continental reconstructions. Terra Cognita 7:99

Smith AB, Xu J (1988) Palaeontology of the 1985 Tibet Geotraverse, Lhasa to Golmud. Phil Trans R Soc Lond A 327:53–105

Taner I, Meyerhoff AA (1990) Petroleum at the roof of the world. The geological evolution of Tibet (Qinghai–Xizang) Plateau. J Petrol Geol 13:157–178, 289–314

Tapponier P, Mercier JL, Armijo R et al. (1981) Field evidence for normal faulting in Tibet. Nature 294:410–414

Wang N (1983) The Tethyan Jurassic stratigraphy of China. Contrib Geol Qinghai–Xizang Plateau 3:62–86

Wang N (1984) Le paléocontinent qingzangindien et sa suturation avec le paléocontinent cathaysien. In: Mercier JL, Li G (eds) Mission Franco-Chinoise au Tibet. Editions du Centre National de la Recherche Scientifique, Paris, pp 33–54

Wang Y, Sun D (1985) The Triassic and Jurassic paleogeography and evolution of the Qinghai–Xizang (Tibet) Plateau. Can J Earth Sci 22:195–204

Wang X, Bao P, Chen K (1987) Ophiolites of Tibet (in Chinese). Region Geol China 3:248–256

Wen S (1984) Stratigraphy Mugaganri region and Tanggula region. In: Stratigraphy of Xizang (Tibetan) Plateau (in Chinese). Science Press, Beijing, pp 186–189, 202–236

Williams H, Turner S, Kelley S, Harris N (2001) Age and composition of dikes in Southern Tibet: new constraints on the timing of east–west extension and its relationship to postcollisional volcanism. Geology 29:339–342

Woodcock NH (1986) The role of strike-slip fault systems at plate boundaries. Phil Trans R Soc Lond A 317:13–29

Xu R-H, Schärer U, Allègre CJ (1985) Magmatism and Metamorphism in the Lhasa block (Tibet): a geochronological study. J Geol 93:41–57

Yin A, Harrison TM (2000) Geologic evolution of the Himalayan–Tibetan orogen. Ann Rev Earth Planet Sci 28:211–280

Yin J, Xu J, Liu C, Li H (1988) The Tibetan plateau: regional stratigraphic context and previous work. Phil Trans Royal Soc Lond A 327:5–52

Yu G, Wang C, Zhang S (1991) The characteristic of Jurassic sedimentary basin of Bangong Co-Dêngqên fault belt in Xizang (in Chinese). Bull Chengdu Inst Geol Miner Resour 13:33–44

Zheng H, McAuley Powell C, An Z et al. (2000) Pliocene uplift of the northern Tibetan Plateau. Geology 28:715–718

Zheng Y, Xu K, Yang et al. (1984) Geological characteristics of ophiolite-melange in Ali region and its relationship with regional tectonics (in Chinese). J Changchun College Geol 4:29–37